EFFECT OF POROSITY AND GLASS CONTENT ON MACHINING OF ALUMINA CERAMICS BY ELECTROCHEMICAL SPARK MACHINING (ECSM)
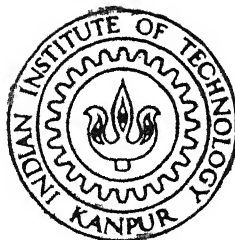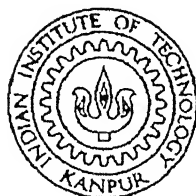
by

Manoj Singh

Department of Materials Science Programme

Indian Institute of Technology Kanpur

July, 1997

EFFECT OF POROSITY AND GLASS CONTENT ON MACHINING OF ALUMINA CERAMICS BY ELECTROCHEMICAL SPARK MACHINING (ECSM)

Thesis Submitted
in Partial Fulfillment of the Requirements
for the Degree of
Master of Technology

by
Manoj Singh

to the
DEPARTMENT OF MATERIALS SCIENCE PROGRAMME
INDIAN INSTITUTE OF TECHNOLOGY KANPUR
July, 1997
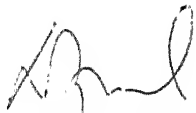
Dedicated to

My Parents

CERTIFICATE

This is to certify that the thesis entitled **EFFECT OF POROSITY AND GLASS CONTENT ON MACHINING OF ALUMINA CERAMICS BY ELECTROCHEMICAL SPARK MACHINING (ECSM)**, by *Manoj Singh* has been carried out under our supervision and this work has not been submitted elsewhere for a degree.
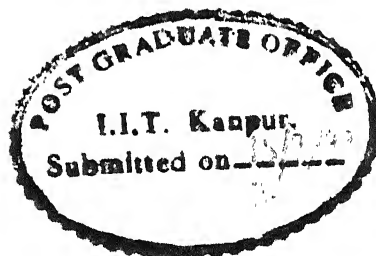
Dr. D. C. Agrawal
Professor
Materials Science Programme
Indian Institute of Technology
Kanpur 208016

Dr. V. K. Jain
Professor
Dept. of Mechanical Engineering
Indian Institute of Technology
Kanpur 208016

July, 1997

POST GRADUATE OFFICE
I.I.T. Kanpur
Submitted on _____

Acknowledgement

I express my deep sense of gratitude to my thesis supervisors Dr. D. C. Agrawal, Professor, Department of Material science, and Dr. V. K. jain, Professor, Department of Mechanical Engineering for Considerate yet rigorous and meticulous guidance. I am deeply indebted to them for their inspiring guidance and constructive criticism and above all for their inspiring devotion throughout the tenure of this work.

I am thankful to Mr. R. M. Jha, Mr. H. P. Sharma, Mr. P. P. Gupta, and Mr. Namdev from Manufacturing Science Lab and Mr. P. K. Paul from ACMS. I would like to express my special thanks to Mr. Atanu Saha (Phd. Scholar) from ACMS and Mr. Manas De and Sunil Jha from Mechanical Engineering Department for their continuous help and constant encouragement.

I am very much thankful to Mr. S. majumdar, Mr. Gurvinderjit Singh, Miss Archana Tripathi and to all who have helped me and make my stay at I. I. T. Kanpur, a memorable one.

At last but not least, I would like to pay my heartly gratitude to my labmates for creating healthy academic environment in the lab.

IIT Kanpur
July, 1997   **Manoj Singh**

Abstract

It has been proposed that one of the mechanisms of material removal in electrochemical spark machining (ECSM) involves melting of the material. In order to test this hypothesis, in the present work alumina (Al_2O_3) samples having different amounts of glass (0% - 20%) are prepared. Machining of these samples is carried out and microstructure of machined and polished surfaces are studied. Process performances e.g., material removal, machined depth and diametral overcut are evaluated. Analysis of the results shows that the machining rate in ECSM process is greatly affected by porosity a of sample. Thus the material removed is found to increase from 6 mg to 110 mg when the porosty increases from 3% to 29%. No clear effect of glass content on MRR is seen. A study of the microstructures of the polished and machined surfaces shows that the material removal occurs by attack at the grain boundaries probably due to an etching process.

Contents

List of Figures

List of Tables

Chapter 1

Introduction

There is a constantly increasing demand for engineering materials having superior properties to those possessed by customary engineering materials. Properties of interest in these materials are ultrahigh strength, high temperature and thermal shock resistance, high fatigue strength, high wear resistance and high strength to weight ratio etc. However high values of these properties make it difficult to shape these materials using conventional methods, thereby limiting their widespread applications. Ceramics have very attractive properties while machining of ceramics by conventional methods is either not possible or uneconomical.

The nonconventional machining techniques being explored for machining ceramics fall into two categories, those in which the consideration of electrical properties of work material is crucial and other which do not depend upon electrical properties of work materials. Techniques like Abra sive Jet Machining (AJM), Laser Beam Machining (LBM), Ultrasonic Machining (USM) and Electron Beam Machining (EBM) fall in the later category but they have their own problems associated with them. For the first category of techniques, Electrochemical Machining (ECM) and Electro Discharge Machining (EDM) are well established.

Lately Electrochemical Spark Machining (ECSM) process is being employed for machining of electrically nonconducting materials like ceramics and composites[1]. ECSM is a hybrid process in which material removal is accomplished by establishing spark in the vicinity of the workpiece.

Mechanism of ECSM is still not very clear however it has been explained as follows :-

1.1 ECD Mechanism And Its Electrical Equivalent

Fig. 1.1 presents a schematic diagram of an ECSM setup. The equivalent electrical circuit of the system is shown in Fig. 1.2.

A simple electrochemical spark machining setup consists of two electrodes dipped in electrolyte, tool is kept as -ve electrode and another electrode of graphite is kept as +ve electrode (Fig. 1.1). When an external potential is applied between the electrodes, the electric current flows through the electrolyte resulting in electrochemical reactions such as anodic dissolution, cathodic deposition, electrolysis of electrolyte etc., depending upon the electrode-electrolyte combination. Electrolytic cell can exhibit any of the following three different phenomenon namely, electrochemical action only, electrochemical action followed by discharge between electrodes, electrochemical action followed by discharge between electrode and electrolyte.If a suitable electrolyte is chosen and electrodes are of grossely different sizes then beyond a certain value of applied voltage, sparks appear at the tool electrode and the currnt drops. This is known as discharge phenomenoa.

The current distribution at the tool electrode is not uniformbecause of the sharp edge at the end face, as a result of which the spark is confined to the iatter region[5].

The current flow at the bottom face area of the electrode is small because of the permanent blanketing by the entrapped gas, and thus can be neglected.

The electrical equivalent of ECD setup is shown in Fig.1.2.In this figure C_1, is capacitance of the circuit, C_2 is the capacitance of the larger electrode- electrolyte interface, C_3 is capacitance of the tool electrode- electrolyte interface due to accumulation of opposite charges at the regions, L is inductance of the circuit, R_1 is resistance at the larger electrode electrolyte interface, R_2 is the resistance of the bulk of the electrolyte, and R_3 is resistance at the tool electrode electrolyte interface.
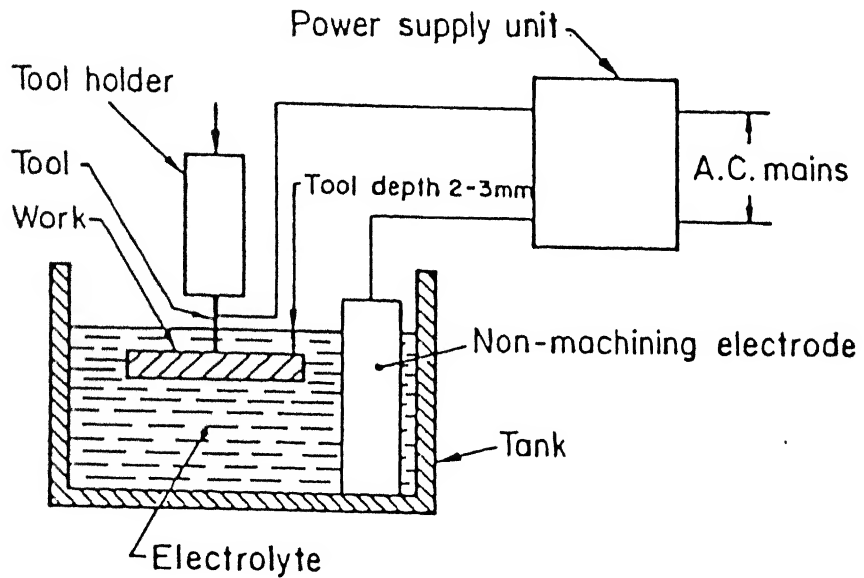
Figure 1.1: Configuration of nonconducting work machining using ECSM [6]

Due to the flow of electric current, hydrogen gas is generated at the cathode (which is used as the tool electrode to avoid electro chemical disolution and subsequent loss of active electrode area) and leads to bubble formation. Bubbles grow in size and
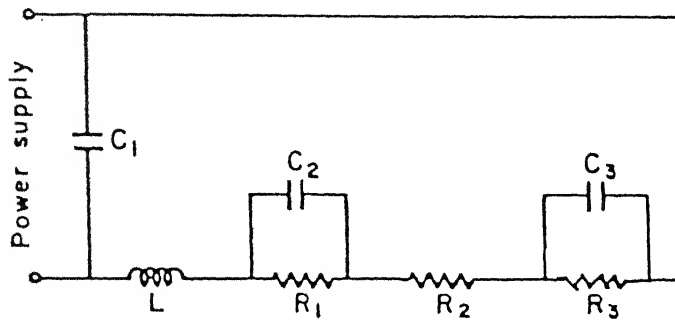
Figure 1.2: Equivalent electrical circuit of ECD setup[6]

once the critical size is reached, detach from the surface and move upwards. When hydrogen bubbles become sufficiently large in number, the resistance of the tool-electrolyte interface increases substantially due to constriction effect. This leads to increased ohmic heating of the electrolyte in this region, causing generation of vapour bubbles. As the current density J increases the number of nucleation sites of bubbles also increases. At the critical condition the number of nucleation sites are such that the fully grown bubbles cover the maximimum possible active surface area of the tool. leading to the blanketing (i.e. isolation between tool and electrolyte). Consequently the current drops to zero in a very small time, which is analogous to a switching off action of an electrical circuit.

It has been observed that sparking occurs at the tool electrolyte interface above a certain voltage depending upon the concentration of electrolye. The sparking is definitely not between the electrodes, rather across a hydrogen gas bubble. If the workpiece is brought in the vicinity of the spark zone, machining would take place[2]. The onset of sparking coincides with the formation of bubbles. Here potential gradient

is more important than the potential difference. In the ECM cell, if the cathode gets covered with a layer of thin large bubbles, the current will be conducted by streamers of electrolyte between the bubbles thus causing a high potential gradient. Due to high potential gradient, breakdown of the gas in a bubble take place and a discharge occurs. The discharge is accompanied by evolution of large amount of heat. The various possible mechanism which may result in the removal of material from the workpiece are as follows.

- Melting and vaporization of the work material

- Mechanical erosion and

- Electrochemical action

The evolution of heat due to sparking has been suggested by many to result in melting and evaporation of work material. Further, mechanical erosion may occur due to cavitation effect of gas bubbles rupturing on the work surface. The discharge through the bubbles will result in a violent rupture. However, the absence of conducting ions in electrically nonconducting work materials helps in concluding that material removal by electrochemical action is not possible. Electrochemical action helps only in generation of bubbles and their evolution at the cathode.

Initiation of spark is somewhat similar to that in electric discharge machining. In the former case, both cations and anions are already present in the electrolyte. Sparking during ECSM would take place only when intervening medium (gas or water vapour bubbles, or passivating layer) is subjected to high electrical pressure that overcomes its insulating properties. A catastrophic current is then allowed to pass through [3]. In ECSM the insulating layer of gas bubbles on the electrodes provides the medium for the initiation of breakdown. A local increase in potential drop on

the film take place, leading to rise in the electric field intensity[4]. At a definite value of electric field intensity, electron conduction results in breakdown and origination of spark dis charge channel. The value of breakdown voltage will depend upon type of electrolyte, the type of gas in the bubbles. The sparking at random location is preferable. Further, the possibility of two consecutive sparks during ECSM taking place at the same place is very low. As soon as the sparking takes place, the bubbles present around the spark will be pushed away by the pressure wave initiated due to sparking and may result in bursting of some of the bubbles. In ECSM, the sparks are desirable not the arcs because the later results in low and localized material removal rate yielding more irregular machined surface.

During sparking as well as no sparking period, the current flows from anode to cathode through the electrolyte. Due to the presence of electrically nonconducting workpiece and supporting plateform, resistance to the flow of current increases. There are two main sources of heat generation during ECSM, i.e., sparking and Joule heating. Only the heat generated due to sparking is productive.

The evolution of bubbles has been observed all around and at the bottom of the cathode . Some of the bubbles merge with others and their size increases to the extent that without sparking they die out [2]. Obviously the smaller size bubbles have higher probab ility of sparking. The energy per spark depends upon size of the bubble, potential difference across the electrodes, electrolyte conductivity and the type of the gas in the bubble. The size of the bubble also plays an important role in determining the material removal rate (MRR). During an attempt to increase the MRR while conducting TW-ECSM exper iments, bubbles of varied sizes were artificially introduced in large number, around the cathode. This resulted in reduced MRR but surface finish improved. In fact, if the artificially produced bubbles merge

with the bubbles generated during ECSM process, the size of the resulting bubble become so high that it dies out without sparking.

It was observed that as the voltage applied across the electrode increased [5], the rate of bubble generation also increased. When the critical value of the voltage was reached, the sparking started at the smaller electrode. Further increase in the voltage, increased the intensity of sparking. Pattern of change in r.m.s. value of current with the r.m.s. value of voltage applied is shown in Fig. 1.3. The sparking starts at V_c and the corresponding current is I_c. The patterns of instantaneous voltage and current variation with time for different regions of the ECD activity are shown in Fig. 1.4 The nature of bubbles distribution on the electrode surface for different values of applied voltage is shown in Fig. 1.5 It is clear that at the onset of sparking the electrode surface is fully covered with bubbles in a closed-packed form.
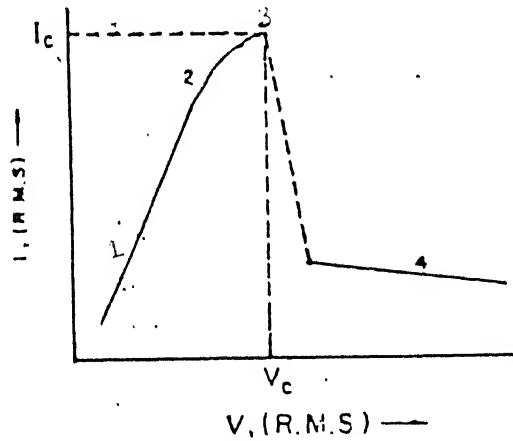
Figure 1.3: Voltage current relationship for a typical ECD cell [5]
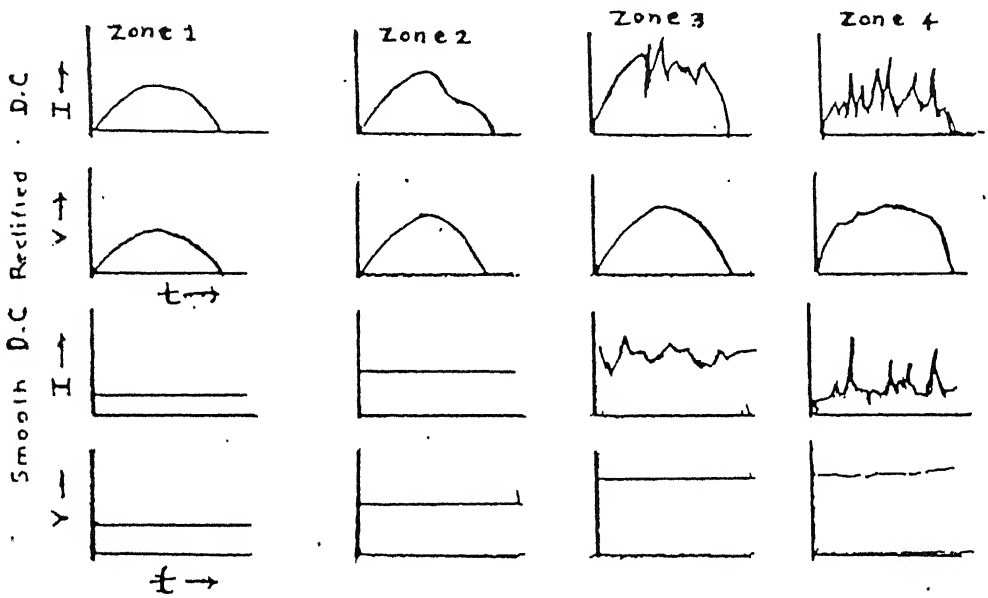
Figure 1.4: Traces of voltage and current for different values of applied potential [5]
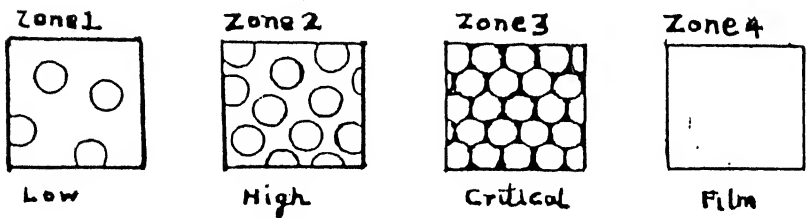
Figure 1.5: Distribution of bubbles for different applied voltage[5]

1.2   Survey Of The Previous Work

Electrochemical spark was first observed by Taylor[11] during electrolysis of molten anode tip and was regarded as "Anode Effect".

In 1950 Kellog[8] also observed the sparks at the cathode, while attempting to enhance of M.R.R. in ECM by the application of higher potential between the electrodes.

In 1968, Kurafuge and Suda[9] utilized this phenomenon of electrical discharge in electrolyte. They used NaOH (15wt%) as electrolyte while making a hole in glass workpiece up to the depth of 0.31mm.

In 1973 Cook et al.[10] conducted experiments based on the process of Electrochemical discharge, while machining glass. They used various fused salts as electrolyte but presumably good results were obtained using an eutectic of NaOH and KOH. They also studied the effect of electrolyte concentration, polarity, cell voltage and temperature of electrolyte and they found that the process is electrolyte sensitive and polarity dependent. They concluded that the best results are obtained with high frequency pulses, although a DC or low frequency AC can also be employed. They showed that machining rate increases with increase in electrolyte cocentration and also with increase in electrolyte temperature, but machining rate decreases with time for a given voltage. Corresponding results are shown in Fig.1.6.

Regarding the mechanism of material removal, they have not been able to establish clearly that wheather it is thermomechanical, chemical, electric field or something else.

In 1984 H.T.Suchiya, T.Inoue and M.Miyazuki[13] used a new method "Wire Electrochemical Discharge Machining" of glasses and ceramics.Work materials used
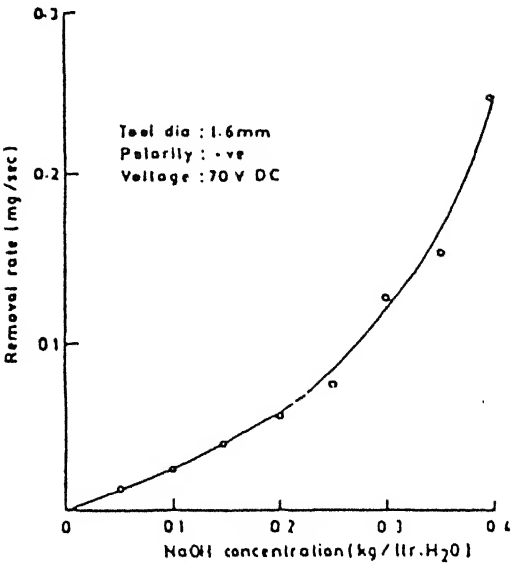
Effect of the electrolyte concentration on removal rate (work material : glass)
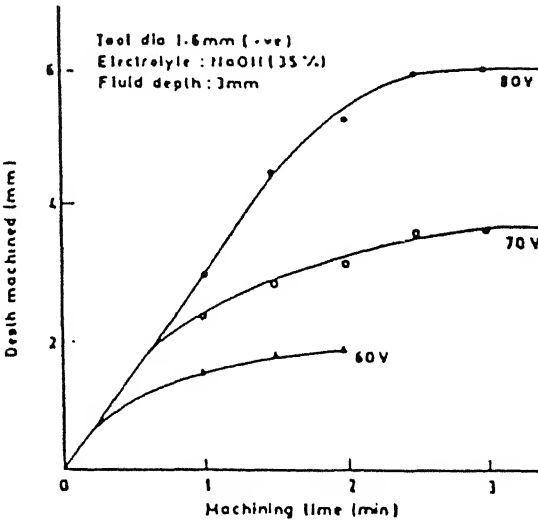
Limited machining depth characteristic (work material : glass)
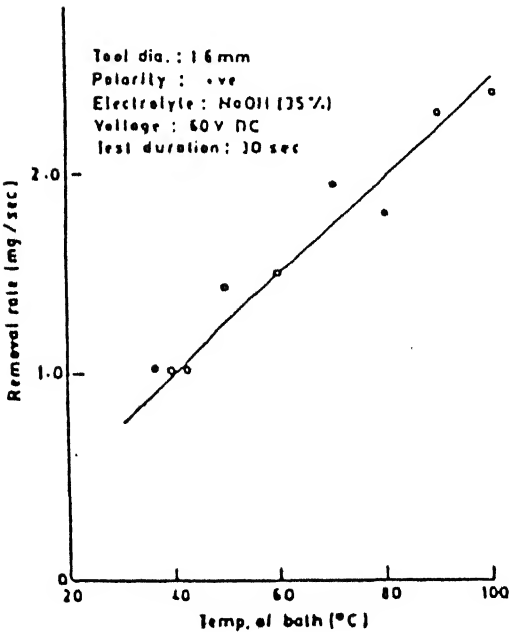
Effect of the electrolyte temperature on removal rate (work material : glass)
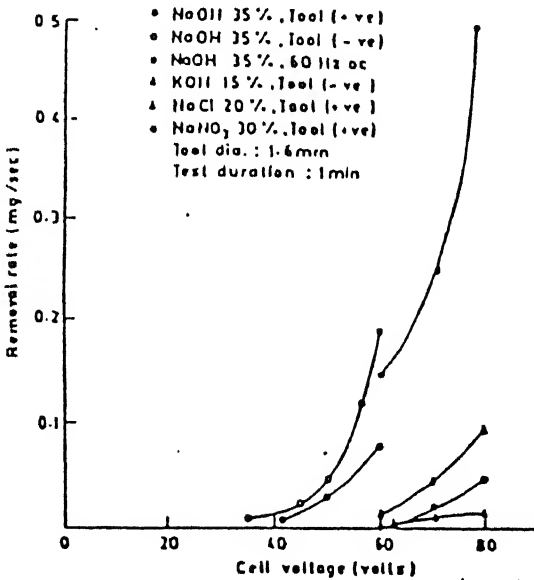
Effect of the applied voltage on MRR (workpiece material : glass)

Figure 1.6: Parametric study of ECDM process during machining on glass [10]

were consists of Soda lime silica, Boro Silicate glass plates, Alumina, Si_3N_4 and SiC ceramic plates. Power supply they have used consists direct current source, a pulse generator and an amplifier.

They examined the effect of polarity of electrode, the electrode voltage, flow rate and concentration of electrolyte on the cutting rate they concluded that cutting rate increases with increasing concentration and voltage (Fig. 1.6) In case of high concentration, the cutting rate rapidly increases with increasing the voltage in case of low concentration cracks generate on the surface of the specimen in high voltage region.

I.M.Crichton, J.A.Mcgeough[12] studied in 1985, the mechanism of discharge in electrochemical arc machining.They reported that electrochemical spark occurs between cathode electrode and electrolyte solution through bubbles formed by electrochemical reaction. On the other hand an arc discharge is formed when spark grows to bridge the gap between the electrodes. Spark discharge has no effect on metal removal while arc discharge leaves a crater on surface.

Allesu et al., made some investigations into spark machining of non conducting materials. They carried out the experiments mainly on glass samples by varying voltage, electrolyte type, electrolyte concentration, electrolyte temperature and also studied the effect of tool size, shape and material on material removal rate. They concluded that with increase in applied voltage m.r.r. increases However beyond a certain value of applied voltage cracks were observed on glass surface. They explained it as due to higher thermal input and subsequent thermal cracking of glass. They used NaCl, NaOH and KOH solutions as electrolytes for evaluating their performance in machining. Among these electrolytes NaOH solution was found to perform better. Regarding the effect of electrolyte concentration on m.r.r., it increases with increase

in concentration. Similarly material removal rate showed a linear relationship with temperature of electrolyte. Higher temperature yielded higher m.r.r. They have also tried tools with different diameters and shapes (solid and hollow) and made of different materials. It was found that lesser the cross-sectional area of tool, better was the performance. Hollow tools gave better performance than solid tools, stainless steel showed very good results as tool material.

Hitoshi Tokura et al [15] carried out electrical discharge in electrolyte to find out the processing method for four kind of ceramics.These ceramics were Alumina and three kinds of Silicon Nitrides series to which are added, Alumina (ASN), Magnesia(MSN), Yttria and Alumina (YASN). The results obtained showed that a pit can be formed on any ceramic and the pit depth apparently varies with the ceramic material. The removal rates of ASN, Alumina, YASN, MSN become low in turn and are independent of their mechanical properties. In case of Silicon nitride series , the removal rates dependent on their sintering additives, and higher the applied voltage, higher the material removed. High removal rate and low electrode loss are obtained when the needle electrode is negative. They used NaOH (20wt%) as electrolyte while machining of all these ceramics. They also showed that minimum voltage necessary to form pit increased with decreasing NaOH concentration. Mechanism of material removal during machining of ceramics was claimed as the etching of grain boundaries in high temperature electrolyte during discharging.

Naveen Gautam [16] did experiments with different tool kinematics like stationary tool, rotating tool with or without electrolyte flow through it, tool with orbital rotation, and upward movement of workpiece. He showed that rotation of tool and flow of electrolyte through the tool have improved the process performance upto some level. He concentrated on Borosilicate glass and did some experiments
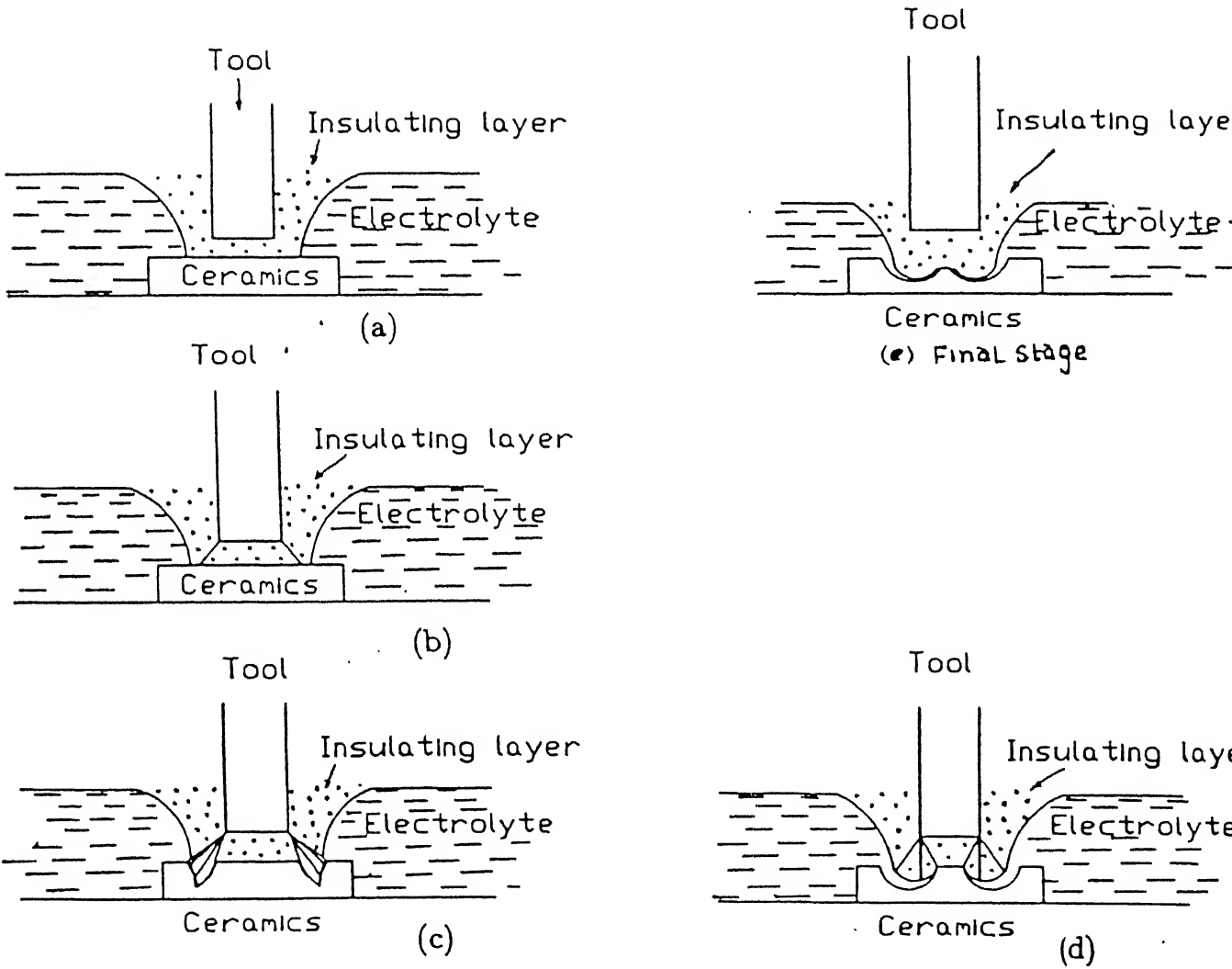
Figure 1.7: Schematic diag. of material removal in Alumina [18]

on Quartz.Through holes were drilled successfully in Quartz glass plates using total discharge configuration.

Raghuram et al [17] studied the effect of various circuit parameters on electrolytes in the electrochemical discharge phenomenon. They showed that external circuit parameters have a definite influence on the discharge characteristics. Internal inductance and capacitance in the electrolytes are observed with the application of rectified and smooth DC voltages. The introduction of an external inductor on the circuit has the advantage of supplying a constant power input to the cell.

I. Basak [18] has done experiments on machining of glass using ECSM process with different electrolyte such as NaOH, KOH NaCl and different power supply such as smooth DC and full wave rectified DC. He showed V-I characteristics for different electrolytes, tool diameter, tool depth and concentration of electrolyte in Fig.(1.7) He showed that MRR can be increased by 200% by introducing inductance into the circuit. He concluded that electrical discharge takes place due to switching action. Singh et al [1] have explored the feasibility of using TW-ECSM process for machining of electrically partially conducting materials like PZT and Carbon fibre epoxy composites. They conducted experiments to investigate the effect of supply voltage and concentration of electrolyte on MRR. MRR is found to increase with increase in supply voltage and electrolyte concentration .

Naotake et al [19] have suggested a new method "Assisting Electrode Method for Machining Insulating Ceramics" for machining nonconducting materials. In this method a metal plate or metal mesh is placed on the surface of the ceramics as an assisting electrode. The ceramics can be easily machined with a copper electrode in sinking EDM configuration or with brass wire in WEDM using kerosene as working fluid. Electrical conductive compound like cracked carbon from working fluid are

generated on the surface of the ceramics. It keeps the electrical conductivity on the surface of the workpiece during the machining .

It is presumed that a conductive layer is continuously generated on the surface of the ceramic EDM process. Therefore, it is considered that when a discharge occurs at a point on the surface of the ceramic the material of the copper from the electrode and carbon from the oil move onto the ceramic surface with larger area than the discharge crater. This is the reason why the machined surface is always covered with conductive materials during the machining.

Lok and Lee [20] have discussed a method "Wire-Cut EDM" process for machining of advanced ceramics. Two type of advanced ceramics, Sialon and Al_2O_3-TiC, were machined successfully by the Wire-Cut EDM process. This process is applicable if the resistivity of the work material is less than a particular threshold value of $100 ohmcm$ and also thermal spalling erosion mechanism of the process was found to have a damaging effect on the surface of the machined ceramics.

Recently Sanjay Chak [7] has done experiments for machining of Alumina and Quartz by ECSM process. He also studied the effect of supply voltage and electrolyte temperature on MRR. They showed in Fig. 1.8 that MRR is found to increase with increase in supply voltage and electrolyte temperature.

1.3   Aim Of The Present Work

One of the mechanisms for material removal proposed by many researchers [7] involves melting and evaporation of material. If so, then the material removal rate should increase greatly if a ceramic contains some amount of low melting phase such as a glass. The problem which we have therefore posed to ourselves is "does the mate-
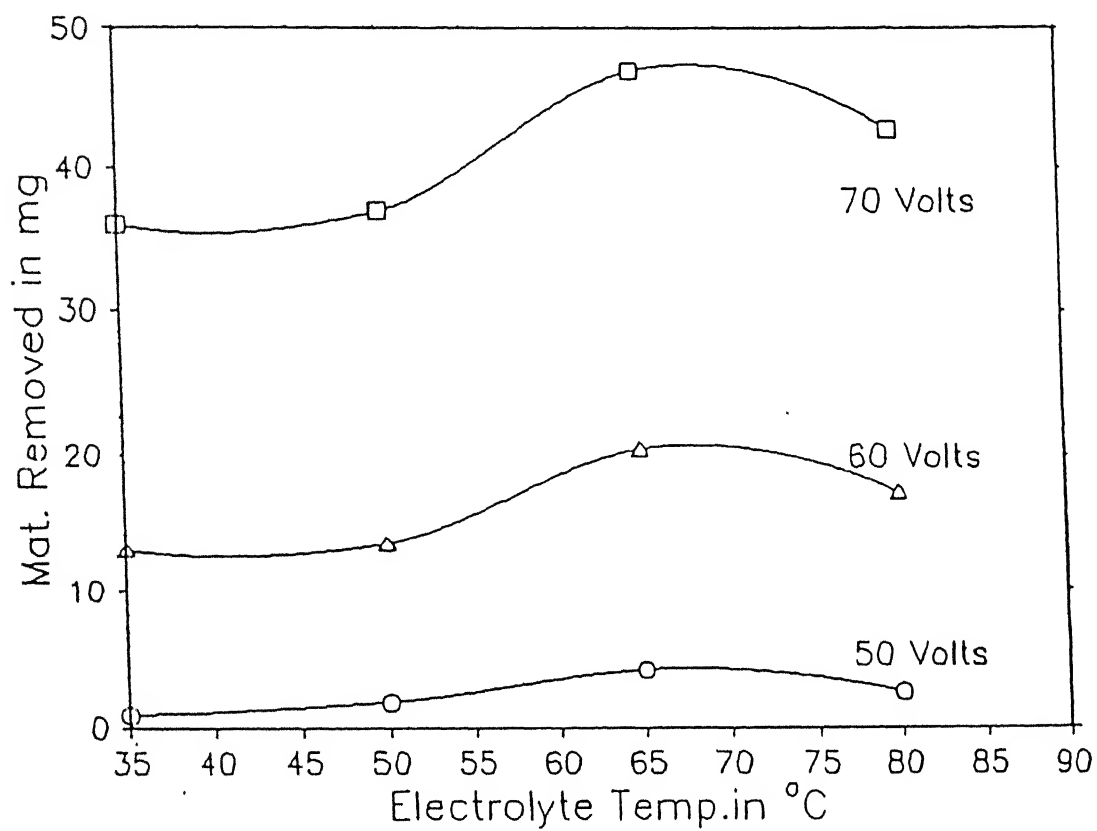
Figure 1.8: Variation of material removed with process variables in Alumina [7]

rial removal rate increases with increasing glass content in ceramic other parameters remaining constant?". If yes, then this should give support to melting mechanism.

To answer the above question, in the preesent work, samples of a ceramic (alumina) with different amount of glass were prepared and their machining by ECSM studied, keeping other factors constant as far as possible.

Chapter 2

Experimentation

2.1   Experimental Set-up

Experimental set-up shown in fig (2.1) is used for Electrochemical Spark Drilling
(ECSD) of ceramics (alumina) designed and fabricated by Gautam [6]. Tool is fitted
on a wirevice which is attached to the bottom portion of adjustable slide. An alu-
minium disc is fitted between wirevice and bottom portion of adjustable slide. Tool
is gravity fed, thus when the tool touches the workpiece, the adjustable slide along
with disc lifts up which presses the microswitch and electrical circuit is completed it
is indicated by lightening of bulb. Thus by reversing the direction of feed motor gap
between the tool and workpiece is set again.

Smooth D.C. power supply is used. Output voltage can be regulated as per our
requirement. Experiments have been done at two different voltages (50V, 60V) using
sodium hydroxide as electrolyte. Temperature of the electrolyte is kept constant at
50 degree centigrade throughout the experiment.

Two independent stepper motors are used with suitable independent "Unistep"
controllers for the drive system. One is used forworkfeed and another is used for tool
rotation. Work feed stepper motor is 12V , 20 kg-cm torque and tool rotation stepper
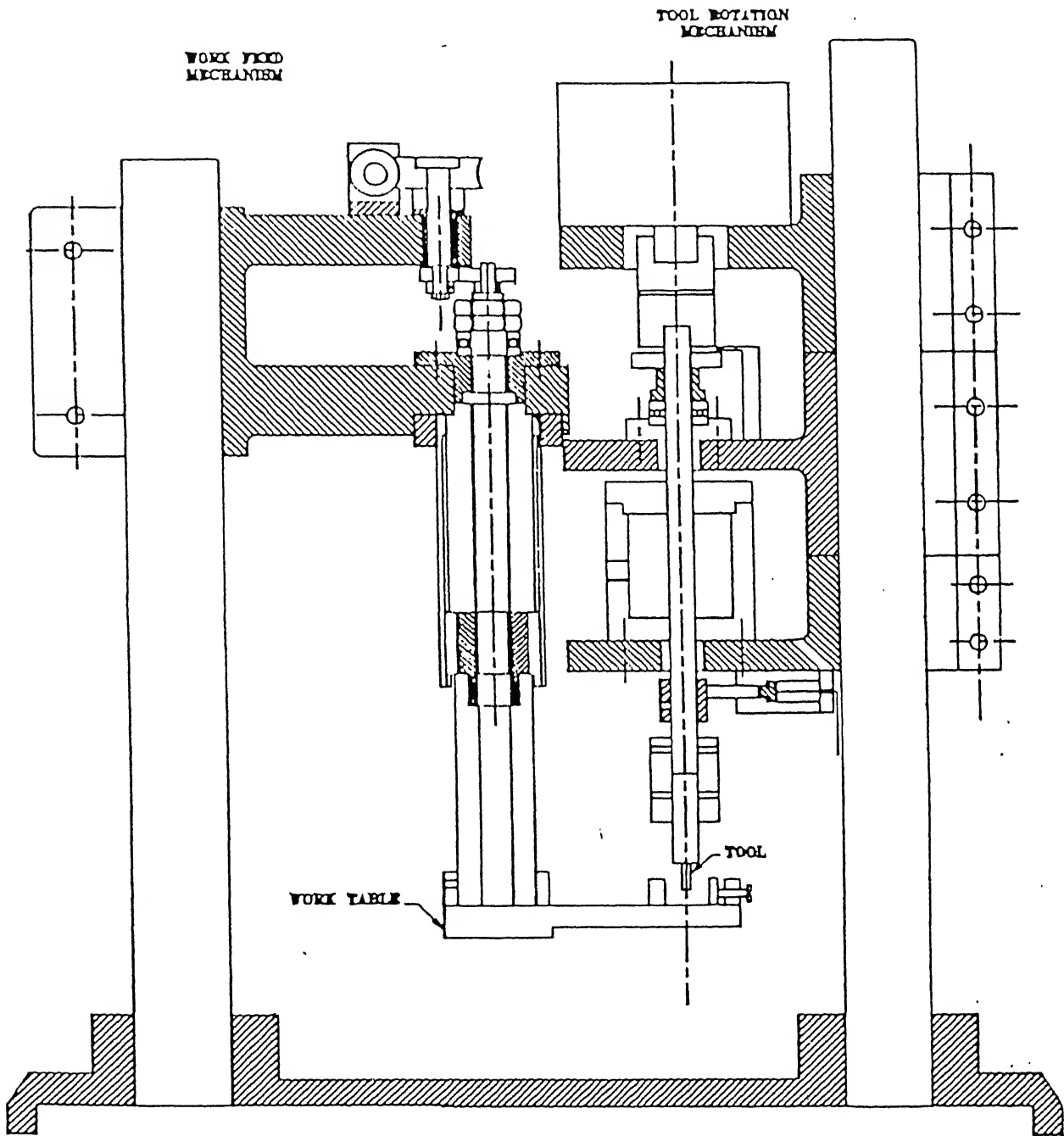
Figure 2.1: Electro chemical spark drilling machine[6]

(b) Tool holding mechanism.

1. SPINDLE
2. STEPPER MOTOR
3. INSULATED CLAW COUPLING
4. MOTOR PLATFORM
5. COLUMN
6. THRUST BEARING
7. COLLAR
8. TEFLON BUSH
9. BEARING PLATFORM
10. BASE
11. ELECTROLYTE CHAMBER PLATFORM
12. CARBON BRUSH
13. BRUSH CASING
14. ELECTRIC CONNECTION
15. SLEEVE
16. TOOL
17. COUPLER
18. ELECTROLYTE CHAMBER
19. MICRO SWITCH

(a) Workpiece holding mechanism.

1. WORK VICE
2. WORK TABLE
3. PERSPEX CYLINDER
4. COLLAR
5. TIGHTENING SCREW
6. SLIDING NUT
7. BRASS CYLINDER
8. LEAD SCREW
9. PLATFORM
10. COLUMN
11. BASE
12. WORM
13. WORM WHEEL
14. GEAR
15. PINION
16. WORM SHAFT
17. BRACKET
18. PIN
19. BUSH
20. THRUST BEARING
21. BUSH
22. CI COLLAR
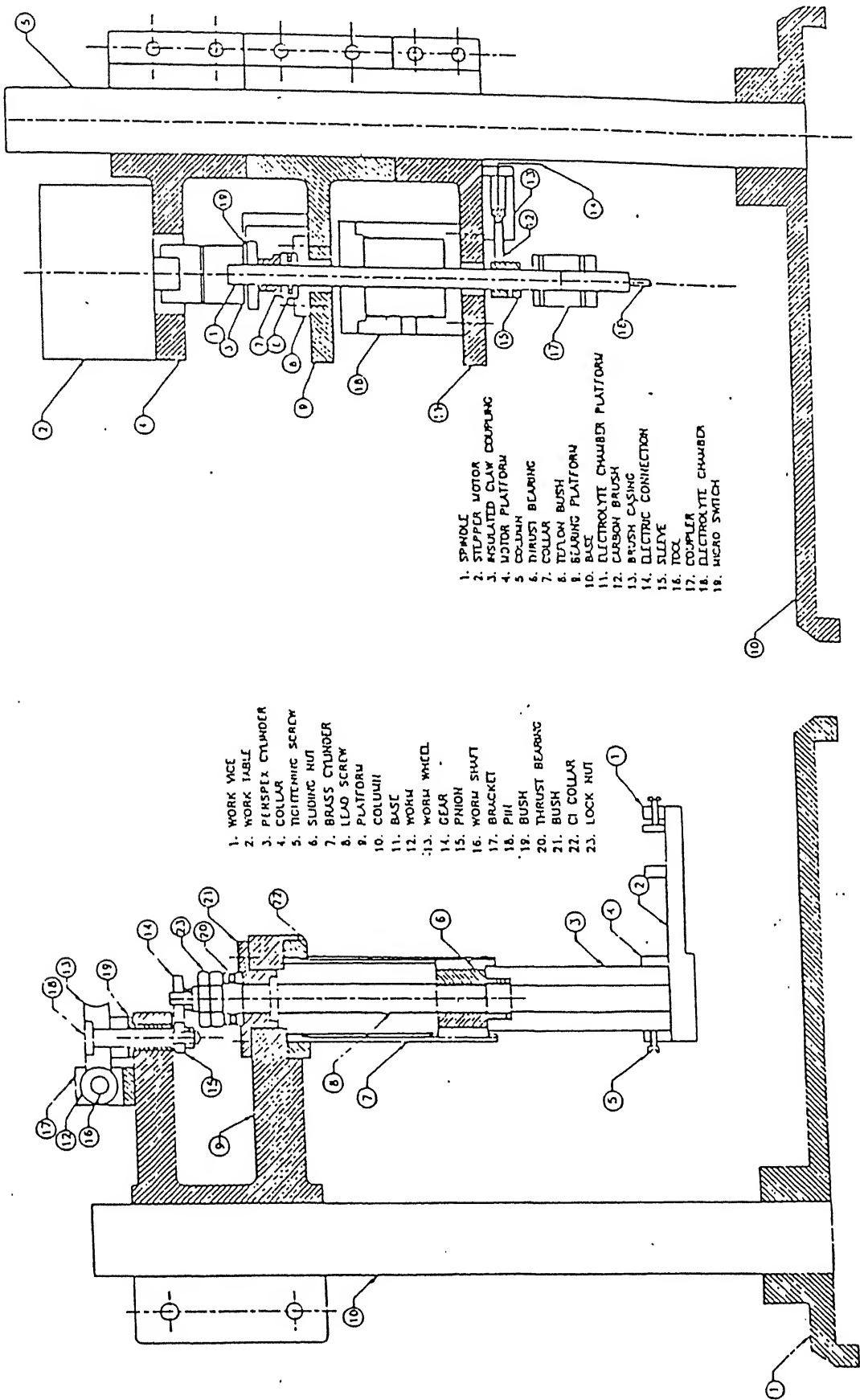23. LOCK NUT

Figure 2.2: Details of electro chemical spark machine [7]

motor is of 12V and 7 kg-cm torque. workfeed motor is connected to wormgear and then with reduction gear(gear ratio 80:1) and with the help of screw and nut mechanism feed is given to the workpiece. Tool rotation motor is directly coupled with hollow pipe whose another end is fixed with adjustable eccentric slide. Beneath this slide a wirevice is attached in which tool is fixed.

2.2   Electrolyte

Throughout the experiments 22 wt% Sodium Hydroxide (NaoH) solution is used as electrolyte because its conductivity is maximium at 22 wt% concentration. As most of the previous work has been done by NaoH and KoH solution, so using NaoH solution as electrolyte will help in comparing the results. NaoH solution is prepared in distill water and allowed to cool down to room temperature in a closed vessel to minimise the evaporation losses, because dilution of NaoH results in exothermic reaction. Conductivity of electrolyte is checked by digital conductivity meter. This conductivity meter is calibrated by the standard known strength solution of Potassium Chloride. Conductivity of NaOH solution is kept constant througout the experiments.

2.3   Sample Prepration

Samples of alumina containing different amounts of glass were prepared. The glass phase was obtained by adding clay and feldspar to alumina powder.

To get the desired specimens, proportions of alumina, clay and feldspar (Table 2.1)were mixed and ground for different periods of time in a planetary mill using agate jar and agate or alumina balls . Total of 20 gm powder is prepared at a time. Purpose of grinding pure alumina for 36 hours using agate balls is to induce

very small amount of glass (from agate) say 0.1$wt\%$ in alumina. After grinding in propanol base, all mixtures are dried in oven at 150^0C and then pressed using 1 wt % solution of polyvinyl alcohol (PVA) as binder in to discs of 15 mm diameter and 3.5 mm height. During pressing the load is kept (600 kg) for one minute.These pressed alumina samples are sintered in a tube furnace at 1450^0c for three hours.

2.4 Electrochemical spark machining

The basic requirements for electrochemical spark machining cell are two electrodes of different polarities and electrolyte . For experimental work, the tool is (copper wire) used as negative electrode and graphite rod as positive electrode. A copper wire of 1.1 mm diameter is used as tool. Tool Rpm is set at 20 for which it gives the maximinum MRR [6]. Tool eccentricity is kept constant throughout the experiments. NaOH 22wt% is used as electrolyte.Workpieces are fastened on workpiecevice and tool is fastened on tool post. Throughout the experiments, the temperature of electrolyte is kept constant at 50^0C with the help of electric heater and thermostate, and is counterchecked by thermometer. The conductivity of NaoH at 50^0C is 490 mmho for 22wt% concentration. Each experiment is carried out for 45 minutes. Level of electrolyte in electrolyte tank is kept fixed by continuously supplying the electrolyte.A minimium level of electrolyte is maintained between tool tip and workpiece.Because downward movement of tool gives spark which results in high overcut on machined surface.
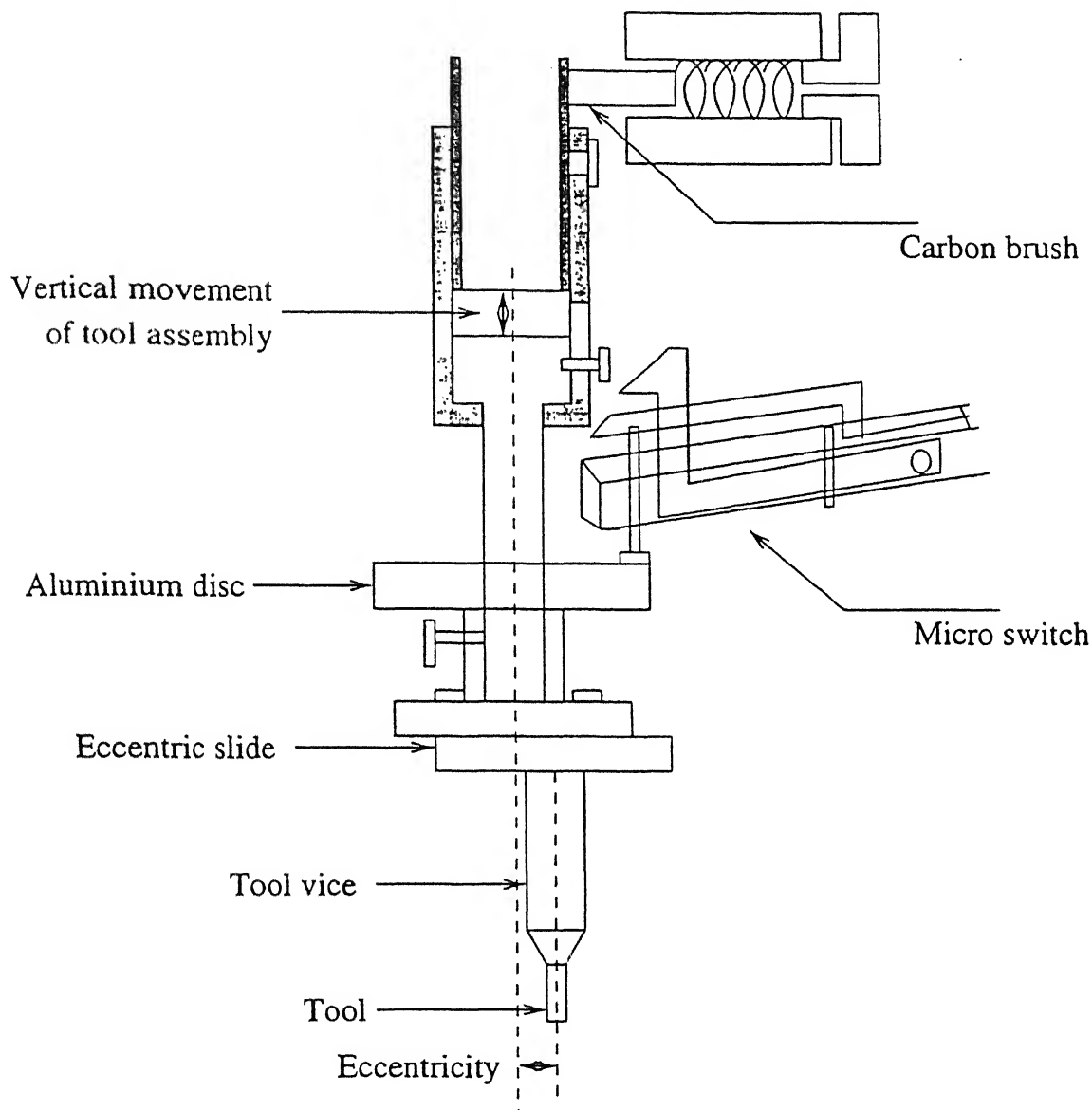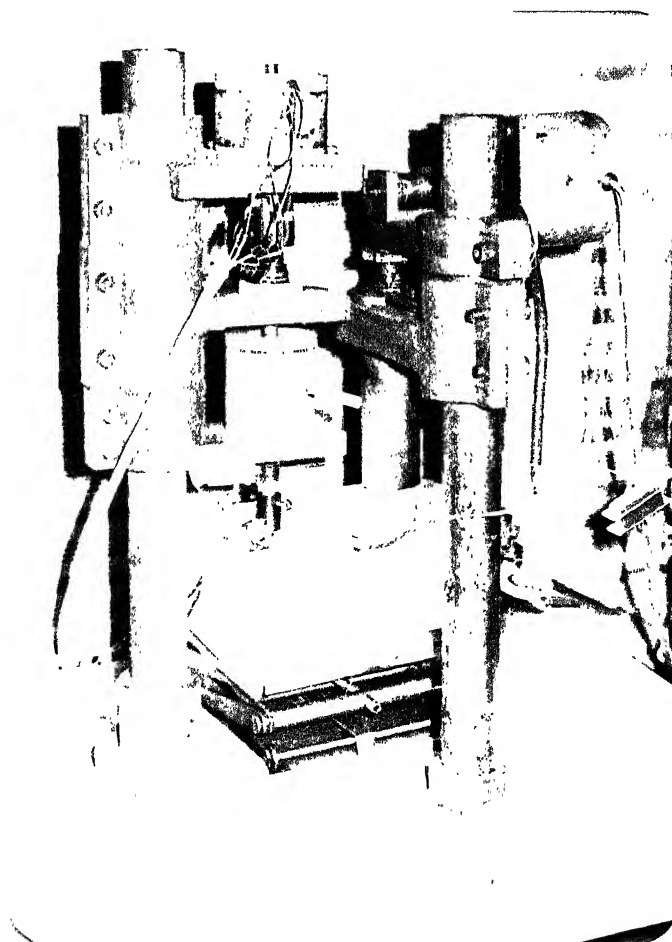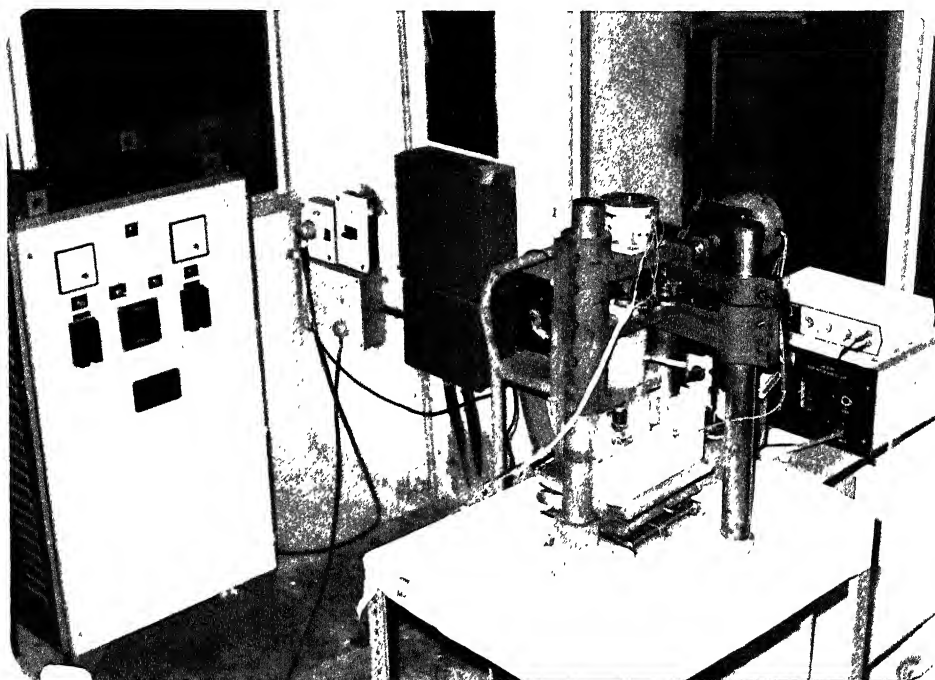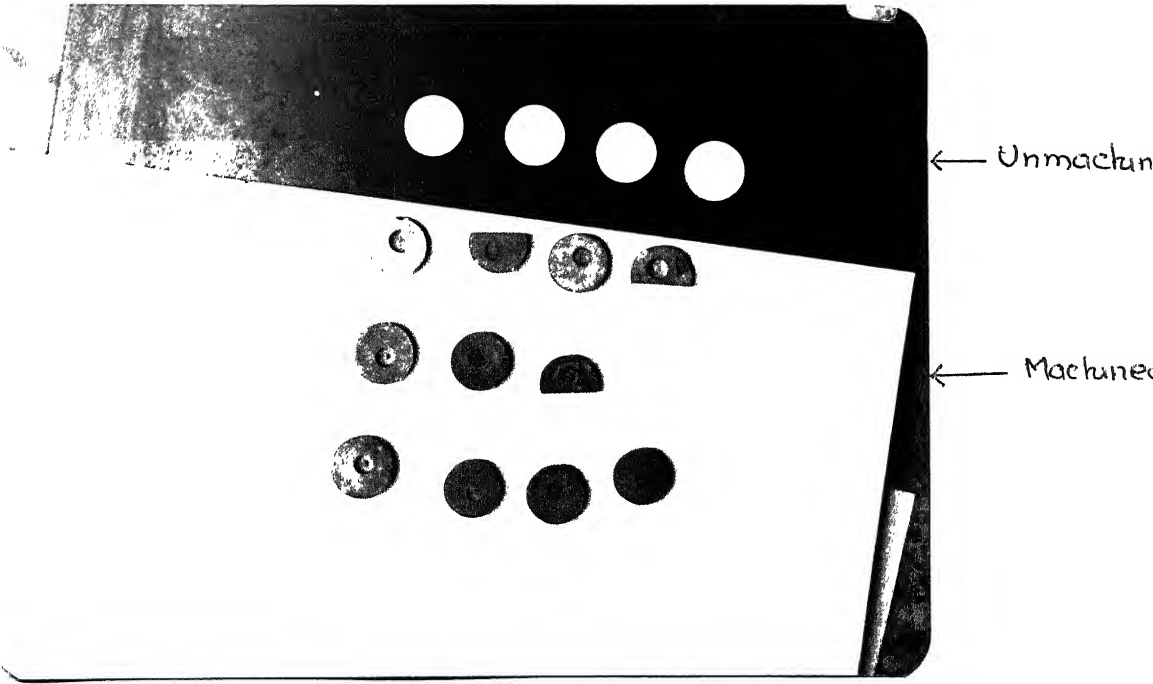
Figure 2.3: Eccentric Tool Mechanism

Figure 2.5: Photographs of machined and unmachined samples

2.5 Measurement Techniques

2.5.1 Material Removal Measurement

For finding out the material removed during machining a workpiece, the difference in weight of the workpiece before machining and after machining is taken. Before taking the weight of sample before machining, it is well cleaned with acetone and then dried. Similarly before taking the weight of the sample after machining, the sample is cleaned by ultrasonic cleaner first in water then in acetone and then after dried .Weight is measured on digitial weighing machine having the accuracy of 0.0001 gm.

2.5.2 Machined Depth Measurement

Machined depth of workpiece is measured by a dial guage whose accuracy is 0.01 mm .Dial gauge is fitted on the stand, workpiece is placed on the plateform. Needle plunger is allowed to rest on unmachined surface and dial gauge reading is taken. Now by suitably moving the workpiece the plunger is allowed to jump inside the machined surface, reading is taken. Difference of these two readings gives the machined depth.

2.5.3 Diametral Overcut Measurement

Overcut on the machined profile is measured using a shadowgraph. The magnified images of machined profiles are analyzed. Overcut is measured by subtracting the tool diameter (d)from the width of the machined profile(w). Width of the machined profile is measured with the help of micrometer attached to the shadowgraph whose acuracy is .001 mm.

Diametral Overcut (O_d) is given as

$$O_d = w - d$$

2.5.4   Surface Integrity and Microstructre

Study of machined and unmachined surfaces of is also carried using scanning electron microscope(SEM).In order to study the machined surface, sample is washed with acetone and dried it is then coated with Au-Pd coating in sputtering unit. To study the unmachined surface , sample is polished subsequently using silicon carbide powder 800 grit size for two hours followed by diamond paste of 3μm , 1μm, 0.25μm for one hour each. After polishing and cleaning, the sample is etched chemically by putting it in a mixture of concentrate HNO_3 and HF in equal amount for five minutes. SEM study of polished surface is carried out to see the presence and distribution of glass in samples.

2.5.5   Differential Thermal Analysis

Differential Thermal Analysis(DTA) of samples is also carried out to see if glass transition could be detected. Rrsults of DTA of the sample (Alumina + 10 wt% glass, two successive runs) are shown in Fig 2.8 and Fig. 2.9. It is difficult to locate the transition temperature T_g from these DTA polts. The small exothermic peaks appear in the plot due to some extraneous matter with which the powder gets contaminated during crushing.
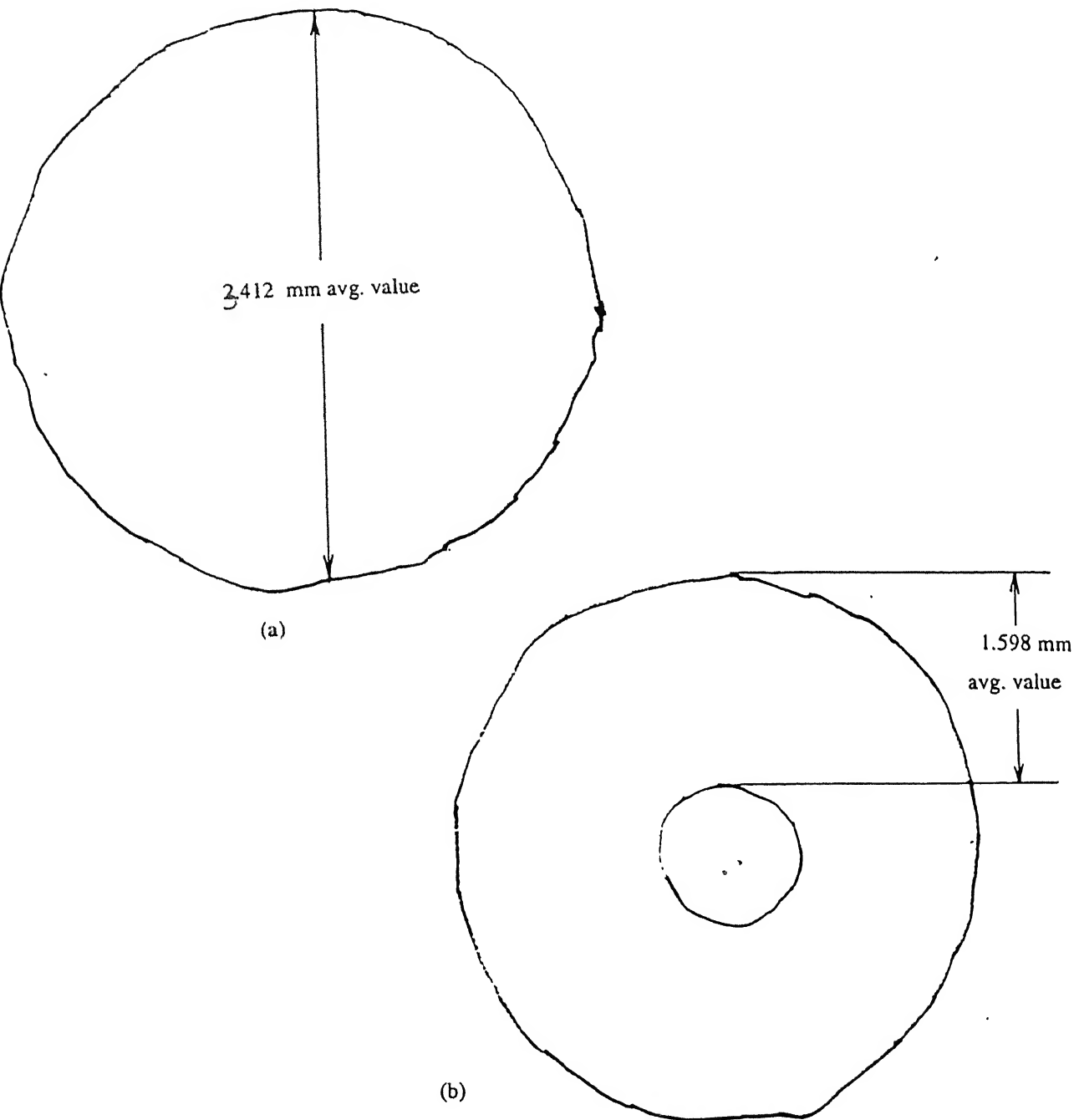
Magnification Scale Common for all Figures

(a)

(b)

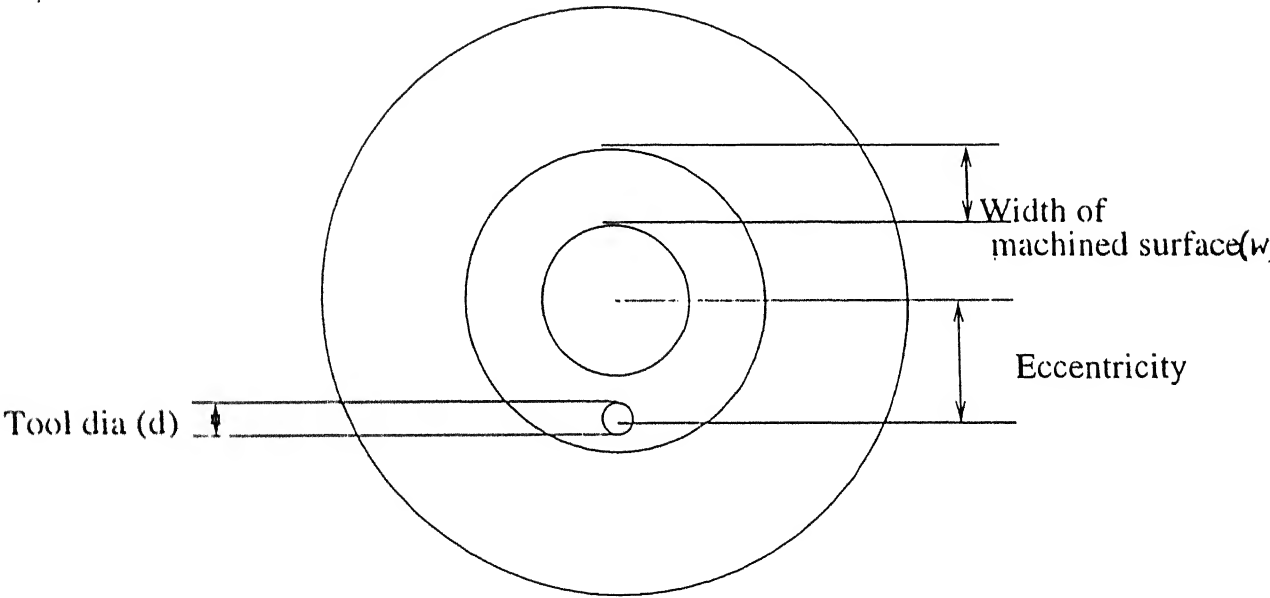Figure 2.6: Shadowgraph picture of samples (a) 2/2 (b) 5/1.See tables 3.1 and 3.2 for details.
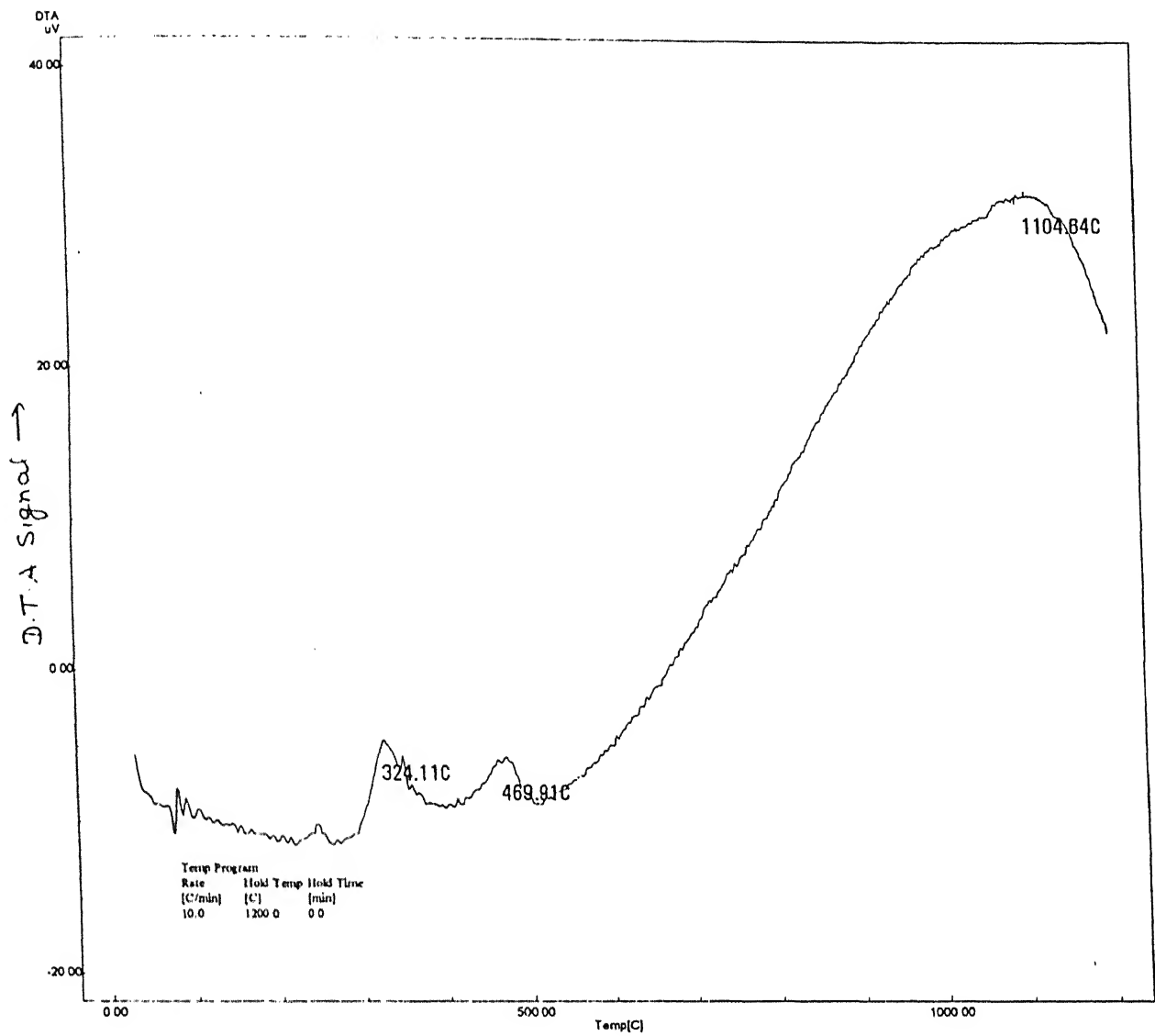
Figure 2.7: Schematic diag. of overcut on samples

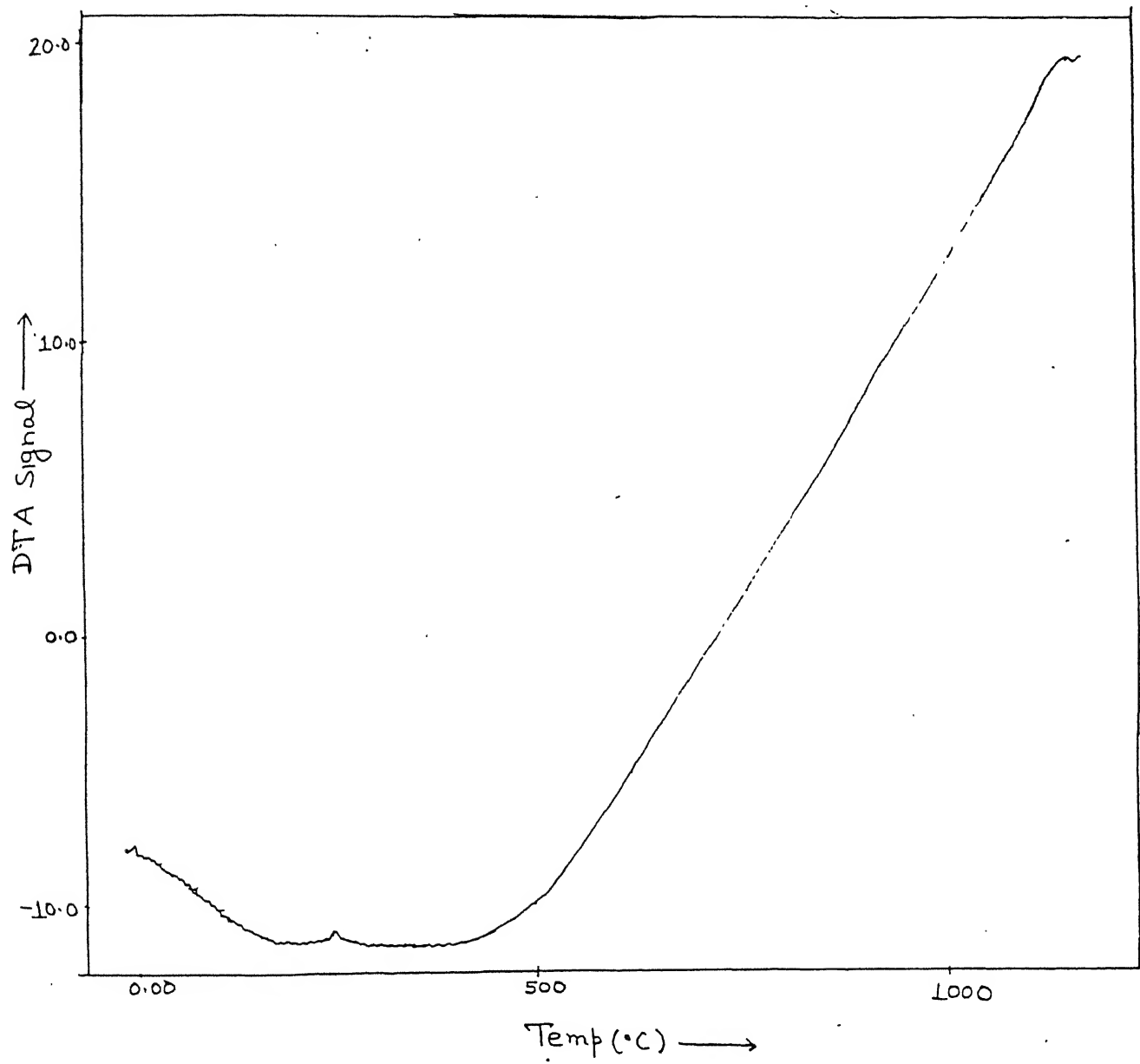Figure 2.8: DTA of sample (Alumina + 10% glass)first run

Figure 2.9: DTA of sample (Alumina + 10% glass)second run

2.5.6 Density Measurement

Density measurement of all these samples is carried out using Archemedes principle by the following procedure.

- Weight of the sample is taken in dry condition.

- All the samples are suspended inside water vessel by tying them with a thin copper wire.

- Water vessel is kept imside dessicator and vacuum pump is operated for one hour to remove the air from pores of samples.

- Weight of samples is taken inside water and in the air.

$$Density = \frac{Dry\ wt\ of\ sample}{[wt\ of\ sample\ in\ air - wt\ of\ sample\ in\ water]}$$

Similarly theoritical density of each sample is calculated using following formula.

$$Theoritical\ Density = \frac{100}{\frac{wt\%\ of\ Alumina}{Density\ of\ Alumina} + \frac{wt\%\ of\ Clay}{Density\ of\ Clay} + \frac{wt\%\ of\ Feldspar}{Density\ of\ Feldspar}}$$

$$\%Density = \frac{Measured\ Density}{Theoritical\ Density} \times 100$$

$$\%\ Porosity = 100 - \%\ Density$$

Density of the samples is measured as per the method explained and results are given in the following table(2.1).

It is evident from the table that the composition which has not been ground has higher density in comparision to the ground sample. Also as the amount of glass is increased, density increased inspite of grinding. Decrease in the density with grinding can be understood by the fact that the reactivity of powder decreases

Table 2.1: Alumina composition and its prepration time

Wt % of Alumina	100	100	99.8	99.2	98.6	98.0	90.0	80.0
Wt % of Clay	0	0	0.1	0.4	0.7	1.0	5.0	10.0
Wt % of Feldspar	0	0	0.1	0.4	0.7	1.0	5.0	10.0
Total glass wt %	0.0	0.0	0.2	0.8	1.4	2.0	10.0	20.0
Theori. Density (gm/cc)	3.98	3.98	3.97	3.96	3.94	3.93	3.75	3.56
Measured Density (gm/cc)	3.860	2.825	3.255	3.306	3.301	3.340	3.375	3.239
% Density	97	71	82	83.5	83.8	85	90	91
% Porosity	3	29	18	16.5	16.2	15	10	9
Grinding Hours	0	36	8	8	8	8	8	8
Grinding Media		Agate balls	Alumina balls	Alumina balls	Alumina balls	Alumina balls	Alumina balls	Alumina balls

due to grinding . The exact reasons for this are not understood. These may involve change in shape and chemistry of the surface of the powder.

Increase in density with increase in amount of glass can be understood by the fact that glass has lower melting point than Alumina. Hence phenomenon of liquid phase sintering take place which results in relatively good sintering and relatively higher density.

Constant Test Conditions During Experimentation

Voltage range = 50 -60

Tool rpm = 20

Tool material = Copper

Conductivity of electrolyte at 50^0C = 390 mmho

Workpiece material = Alumina

Tool eccentricity = 1.5 mm(dia.)

Tool diameter = 1.1 mm

Time of each experiment = 45 minutes

Chapter 3

Results and Discussions

This chapter deals with the experimental observations related to sample preparations, their density measurements and ECSM process. Some work has already been done in the past in the similar area. However, the work reported in this thesis is different from the work done by earlier researchers,

from following view points:

- Alumina samples are prepared by introducing the desired amount of glass in order to study the effect of glass on machining rate and also to find out the exact mechanism of material removal.

- Concentration of electrolyte (NaOH) is kept at 22 wt% for which the conductivity of the electrolyte is maximum.

- A constant gap between tool and workpiece is maintained by using microswitch.

Experiments have been conducted on alumina samples having different amount of glass. During experimentation, the variables used are input voltage, amount of glass, porosity of samples. The detailed observations made in each case are reported below.

3.1 Machining of Alumina

3.1.1 Effect of Glass Content

The effect of glass has been studied on the following responses :

- Material removed from samples,

- Machined depth achieved in samples and,

- Diametral overcut obtained on the machined profile

Material Removal

Material removed from a workpiece is measured in terms of weight loss as explained in chapter 2. It is observed that material removal during machining is increased (Fig. 3.1) when glass content varies from 0 wt % to 0.1 wt % and after that material removal decreases with increase in the amount of glass. But when amount of glass becomes quite significant say about 10 wt % then amount of material removed becomes almost independent of amount of glass . Maximum material removed is achieved as 110 mg.

Tool dia	=	1.1	mm	Voltage	=	60	V
Tool material	=	Copper		Conductivity	=	490-496	mmho
Tool rpm	=	20		Electolyte conc	=	22	wt %
Tool eccentricity	=	1.5	mm	Electrolyte temp	=	50	^{0}C
Machining time	=	45	min				

Constant machining conditions during experiment

Machined Depth in Workpiece

Machined depth in workpiece is maesured with the help of a dial gauge shown in Fig 3.2 . The variations in machined depth with the amount of glass is shown in Fig 3.3 .Maximium machined depth achieved is 2.14 mm . In sample of pure alumina
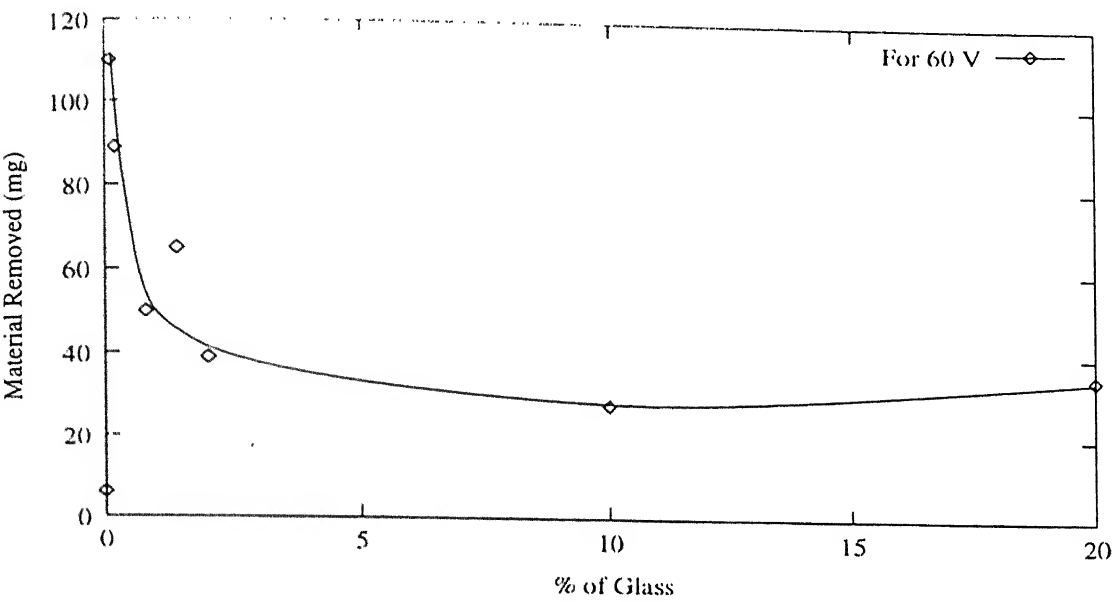
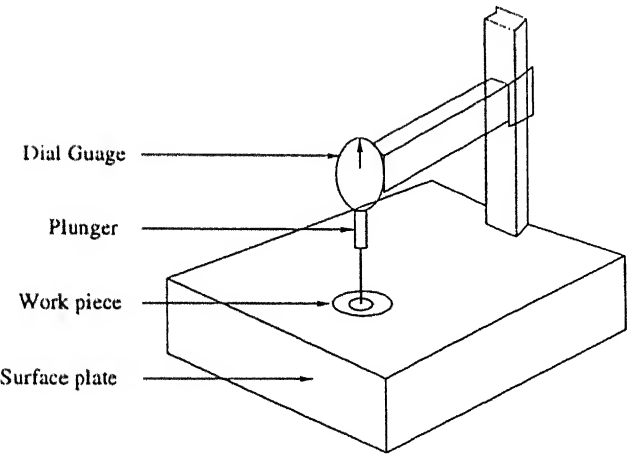Figure 3.1: Variations in material removal with % of glass

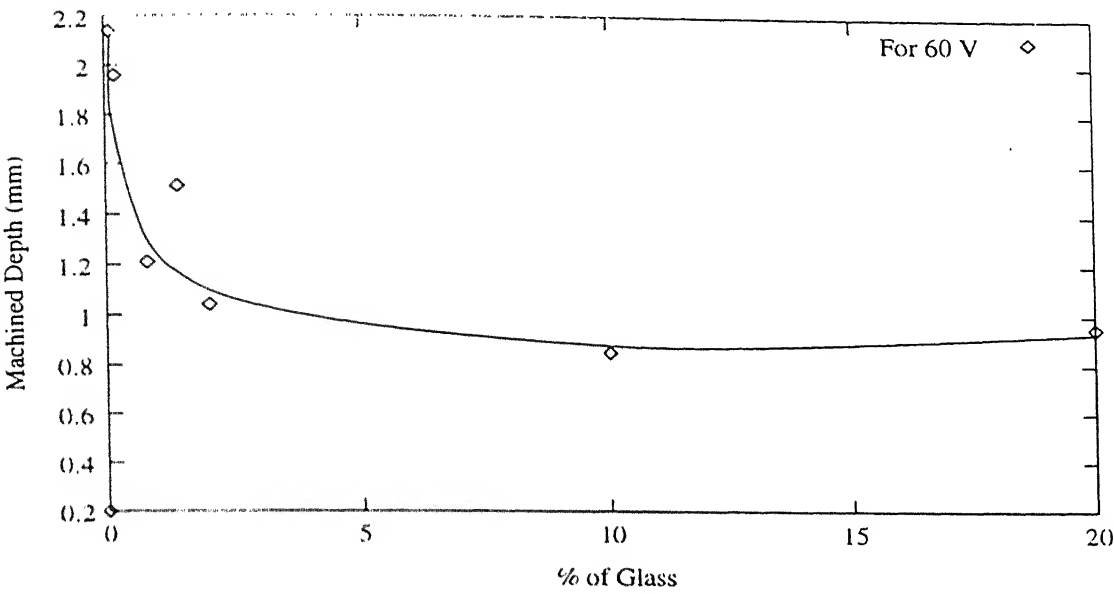Figure 3.2: Set up for machined depth measurement

Figure 3.3: Variations of machined depth with % of glass

ground for 36 hours. Plot of machined depth Vs % of glass shows that machined depth increases from 0 wt% of glass to 0.1 wt% of glass and then decreases upto 10 wt % of glass. For higher amount of glass compositions machined depth remains independent of the amount of glass.

Diametral Overcut

Overut on the machined profile is measured using a shadowgraph.Magnified view of machined profile is analysed and results are shown in Fig 3.4

3.1.2   Effect of Porosity

The effects of porosity on the following responses have been studied while ECSM of alumina.

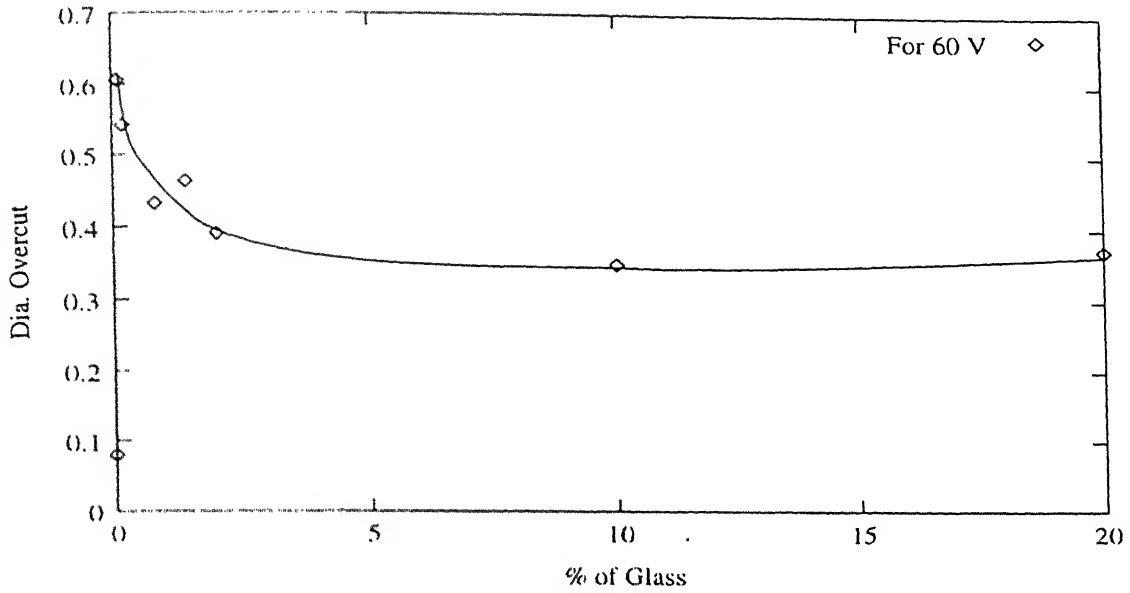- Material removal from the workpiece

Figure 3.4: Variations in diametral overcut with % of glass

- Machined depth achieved in the workpiece, and

- Diametral overcut on the machined profile

Material Removal

Effect of porosity on material removed is shown in Fig 3.5. It indicates that as porosity increases material removal also increases. This increases is very sharp when porosity increases from 15% to 20%, after that increase in material removal with porosity is slow. Maximimum material removal is 110 mg.

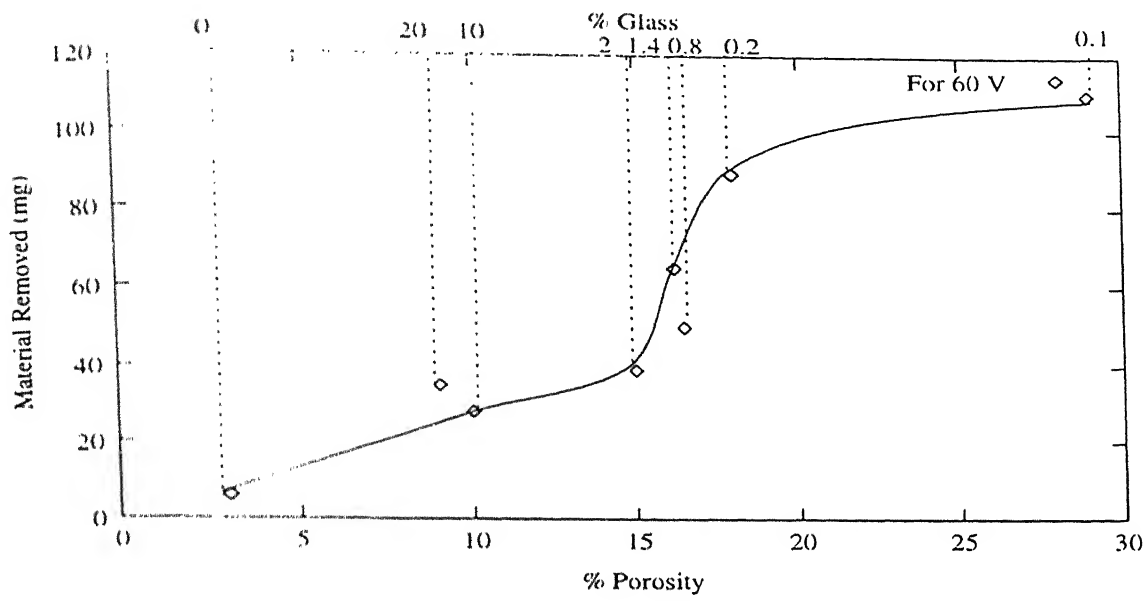| Tool dia.	=	1.1	mm	Electrolyte temp.	=	50	^{0}C
Tool material	=	Copper		Machining time	=	45	min.
Tool rpm	=	20		Conducctivity of elect.	=	490-496	mmh
Eccentricity	=	1.5	mm	Voltage	=	60	V
Electrolyte conc.	=	22	wt %				

Figure 3.5: Variations in material removal with % porosity

Machined Depth

Efffect of porosity on the machined depth is shown in Fig 3.6. Machined depth increases with increase in porosity. Maximium machined depth is achieved as 2.14 mm when the porosity is maximum.

Diametral Overcut on Machined Profile

Study of overcut by shadowgraph shows that with increase in porosity diametral overcut also increases. Response is shown in Fig 3.7.

3.1.3   Effect of Supply Voltage

Effect of supply voltage has been studied on the following responses
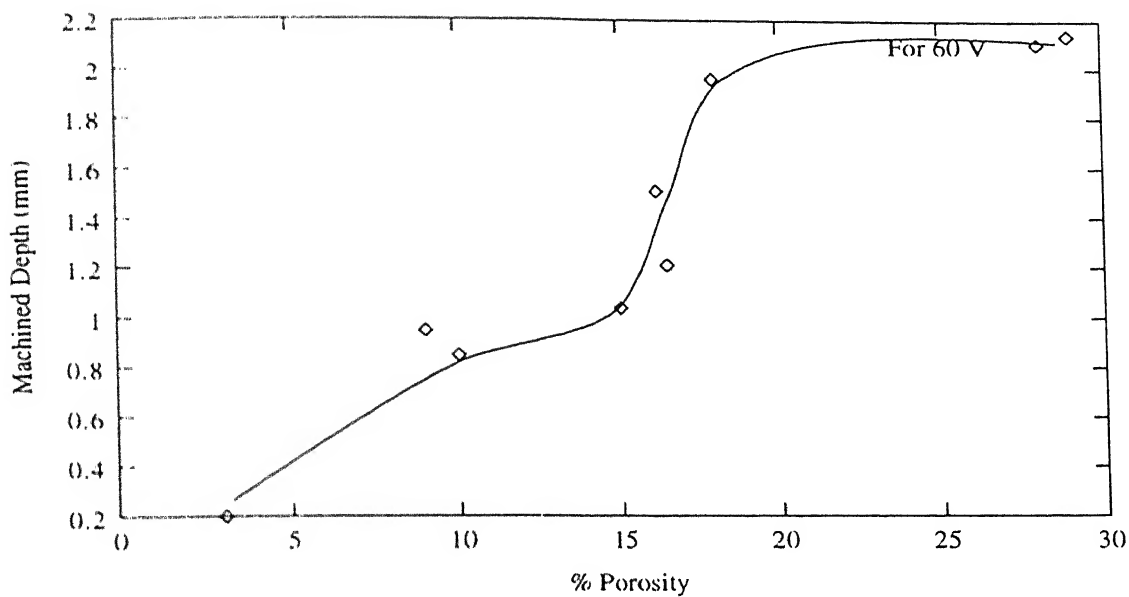
- Material removal

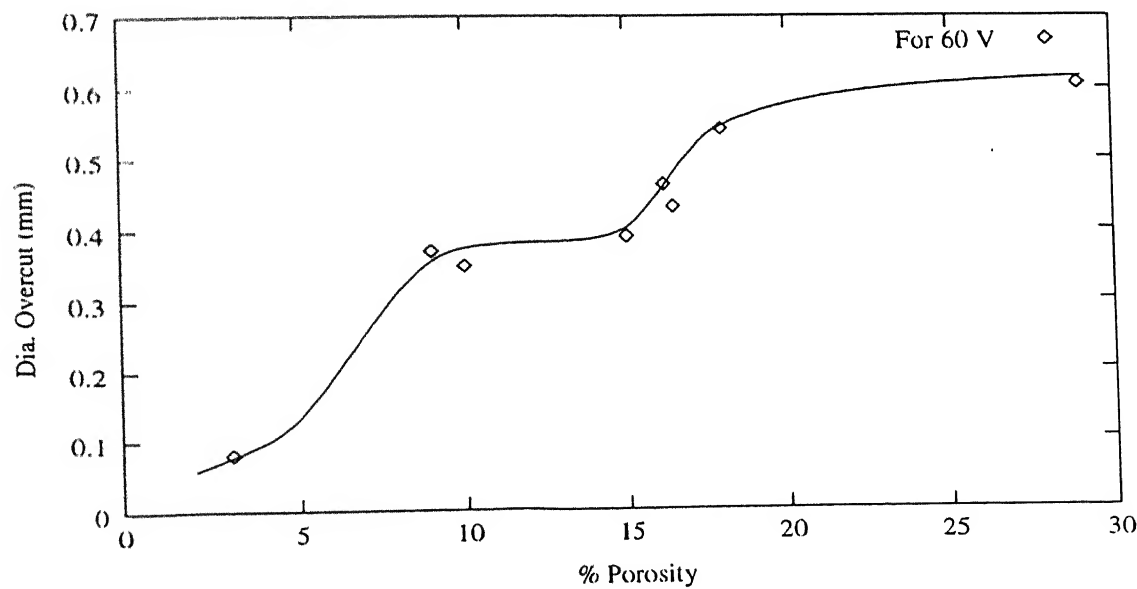Figure 3.6: Variations in machined depth with % porosity

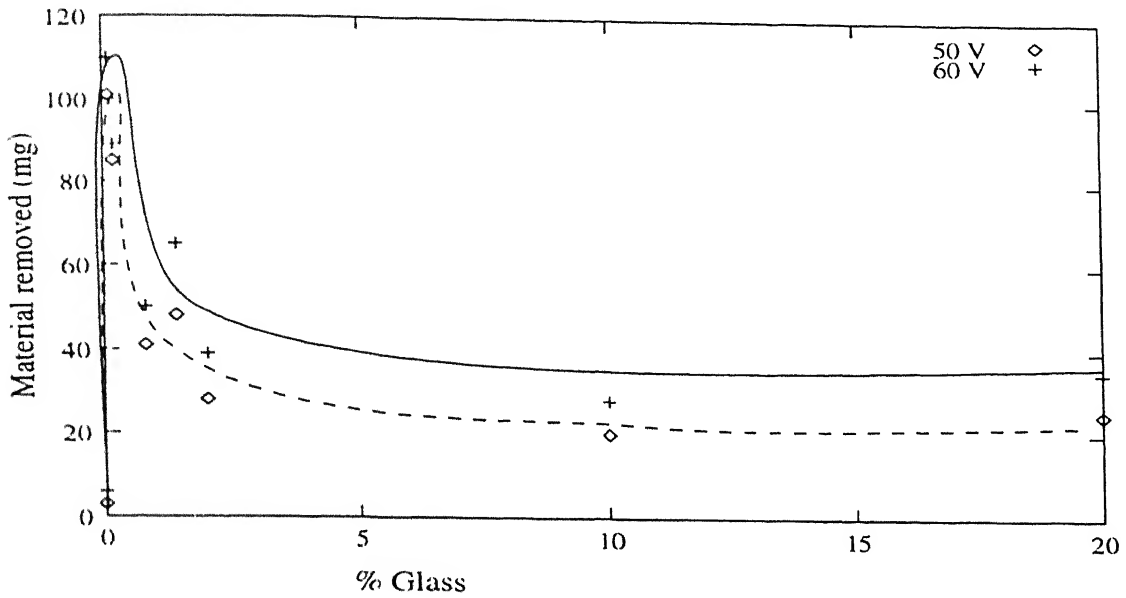Figure 3.7: Variations in diametral overcut with % porosity

Figure 3.8: Variations in material removed with % of glass

- Machined depth and

- Dimetral overcut

Material Removal

Alumina samples of different glass content are machined at two different voltages (50V,60V). Values of material removed are found higher for higher voltage, keeping other parameters (i.e.% of glass and porosity) same. Responses are shown in Fig 3.8 and Fig 3.9 .

Machined Depth in Workpiece

Machined depth in alumina samples is found to be increased with increased supply voltage. Responses are shown in Fig 3.10 and Fig 3.11 .
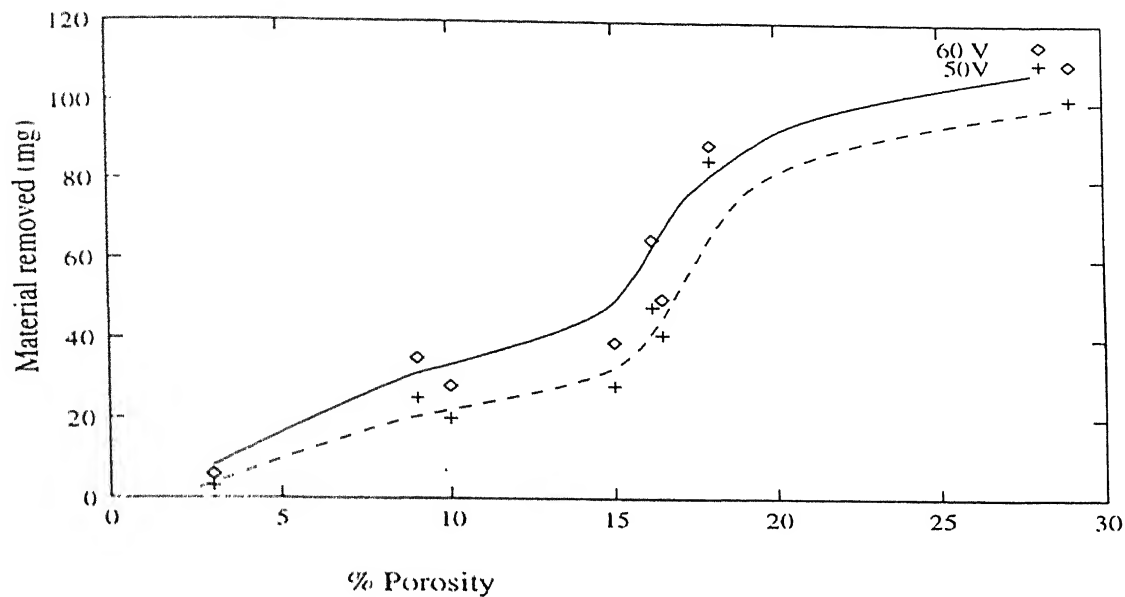
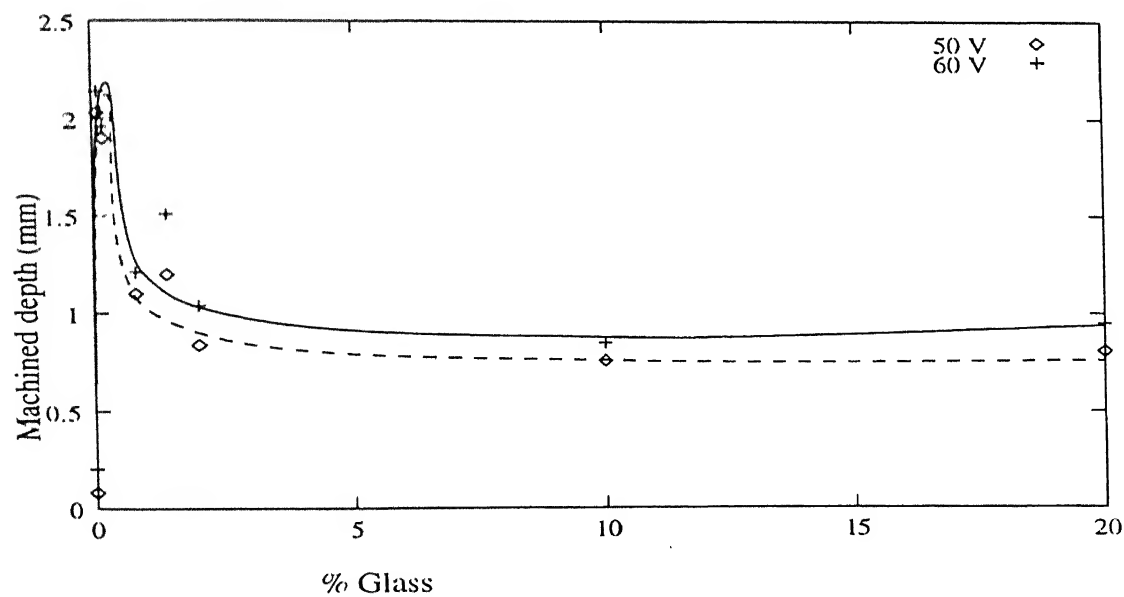Figure 3.9: Variations in material removed with % porosity

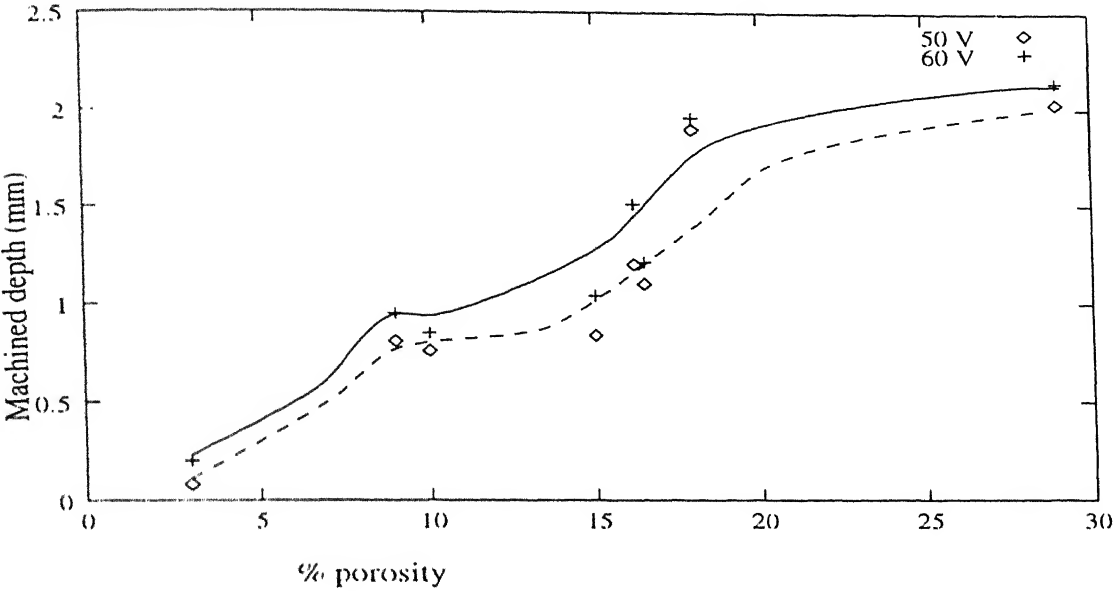Figure 3.10: Variations in machined depth with % of glass

Figure 3.11: Variations in machined depth with % of porosity

Dimetral Overcut in Workpiece

Overcut measured by shadowgraph shows that as the voltage is incrased the dimetral overcut also increased . Various responses are shown in Fig 3.12 and Fig 3.13.

3.2 Tables Showing Various Machining Performances

3.3 Surface Integrity and Microstructure

Various photographs of machined profile, machined surface and polished surface are taken by scanning electron microscope (SEM). Fig 3.14 shows the microstructure of polished surfaces. The pure unground sample (Fig.3.14 a) has large grains indicating that sintering has proceeded to considerable extent. This sample shows the highest density (97 %). The pure ground sample (Fig 3.14b) has most of the grains close
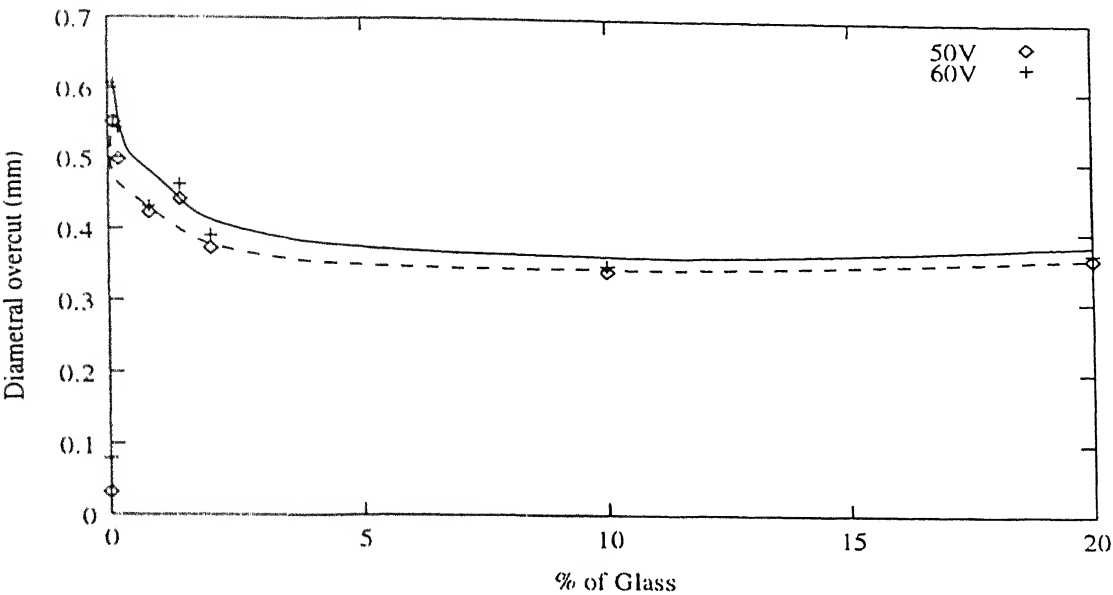
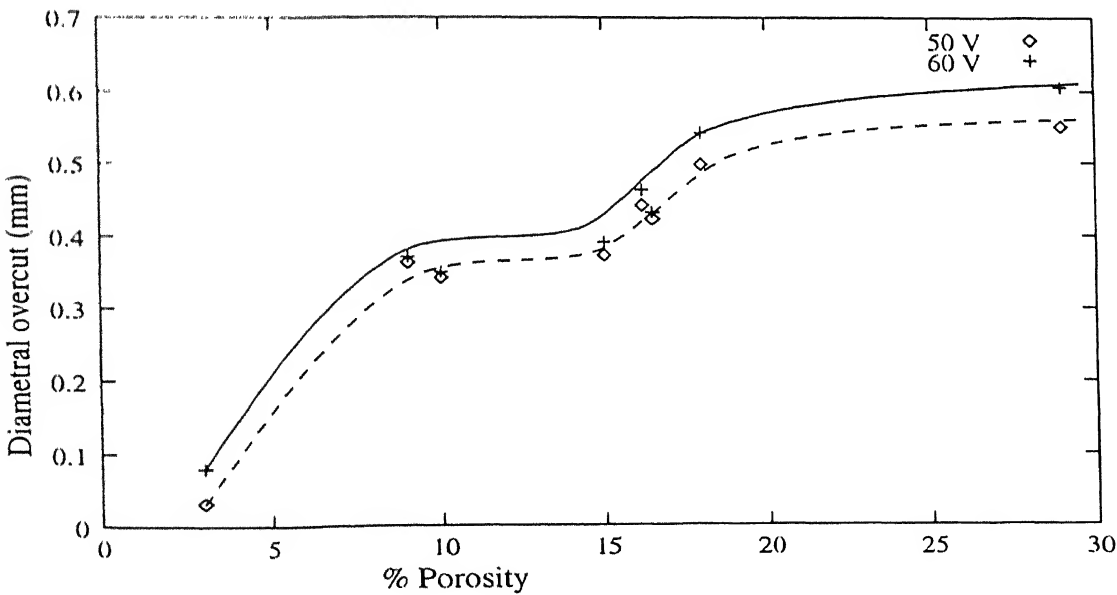Figure 3.12: Variations in diametral overcut with % of glass

Figure 3.13: Variations in diametral overcut with % of porosity

Table 3.1: Values Corresponding to 50^0C and 50V

Sample No.	1/1	2/1	5/1	7/1	8/1	6/1	3/1	4/1
wt % of glass	0	0	0.2	0.8	1.4	2.0	10.0	20.0
Grinding hours	0	36	8	8	8	8	8	8
% Porosity	3	29	18	16.5	16.2	15	10	9
Material removed (mg)	3	101	85	41	48	28	20	25
MRR (mg/min)	0.06	2.24	1.88	0.91	1.06	0.62	0.45	0.55
Avg. machined depth(mm)	0.08	2.03	1.90	1.10	1.20	0.84	0.76	0.81
Diametral overcut(mm)	0.032	0.551	0.498	0.423	0.442	0.373	0.342	0.388

Table 3.2: Values Corresponding to 50^0C and 60V

Sample No.	1/2	2/2	5/2	7/2	8/2	6/2	3/2	4/2
wt % of glass	0	0	0.2	0.8	1.4	2.0	10.0	20.0
Grinding hours	0	36	8	8	8	8	8	8
% Porosity	3	29	18	16.5	16.2	15	10	9
Material removed (mg)	6	110	89	50	65	39	28	35
MRR (mg/min)	0.13	2.45	1.97	1.11	1.44	0.87	0.63	0.78
Avg. machined depth(mm)	0.20	2.14	1.96	1.21	1.51	1.04	0.85	0.95
Diametral overcut(mm)	0.080	0.606	0.542	0.432	0.463	0.391	0.350	0.371

to the starting size (0.3 μm) of alumina. There is substantial porosity between the grains. This sample has the lowest (71 %) density. The microstructure of samples with glass addition show that the liquid phase sintering has taken place and that the distribution of glass is nonuniform. Liquid phase sintering is revealed by the presence of of many grains close to the original particle size (0.3 um) (Fig 3.14 c & d); solid state sintering should result in grain growth throughout the samples. The figures show large clumps which are alumina particles embedded in glass. Thus the glass distribution is nonuniform.

Fig 3.15 to 3.17 show the microstructure of the machined surfaces. Various features are observed. However, an important insight is obtained by comparing the pure alumina, unground sample with other samples. The microstructural features in the pure unground sample (Fig 3.15 a) are of the order of 1 to 2 μm , same as the grain size of this sample (Fig 3.14 a) while those in the 20% glass sample (Fig 3.17 e) are of the order of 0.3 μm, the original particle size of alumina. Similar is the case for samples with other glass contents.As mentioned earlier, the grain size in the (alumina + glass) samples remain close to that of the original alumina particle size because of liquid phase sintering. Thus the conclusion is that in both cases the material is removed by attack on the grain boundary.

The cuboid shaped (Fig 3.17 d & f) and "rosette" like features are occasionally observed (Fig 3.16b,3.17e). These may be a particles of crystalline phase forming due to reaction between alumina, feldspar and clay. However, this needs to be confirmed. Thus from the microstructure it can be said that the material removal is primarily by grain boundary attack. No clear evidence of melting of the material is obtained.
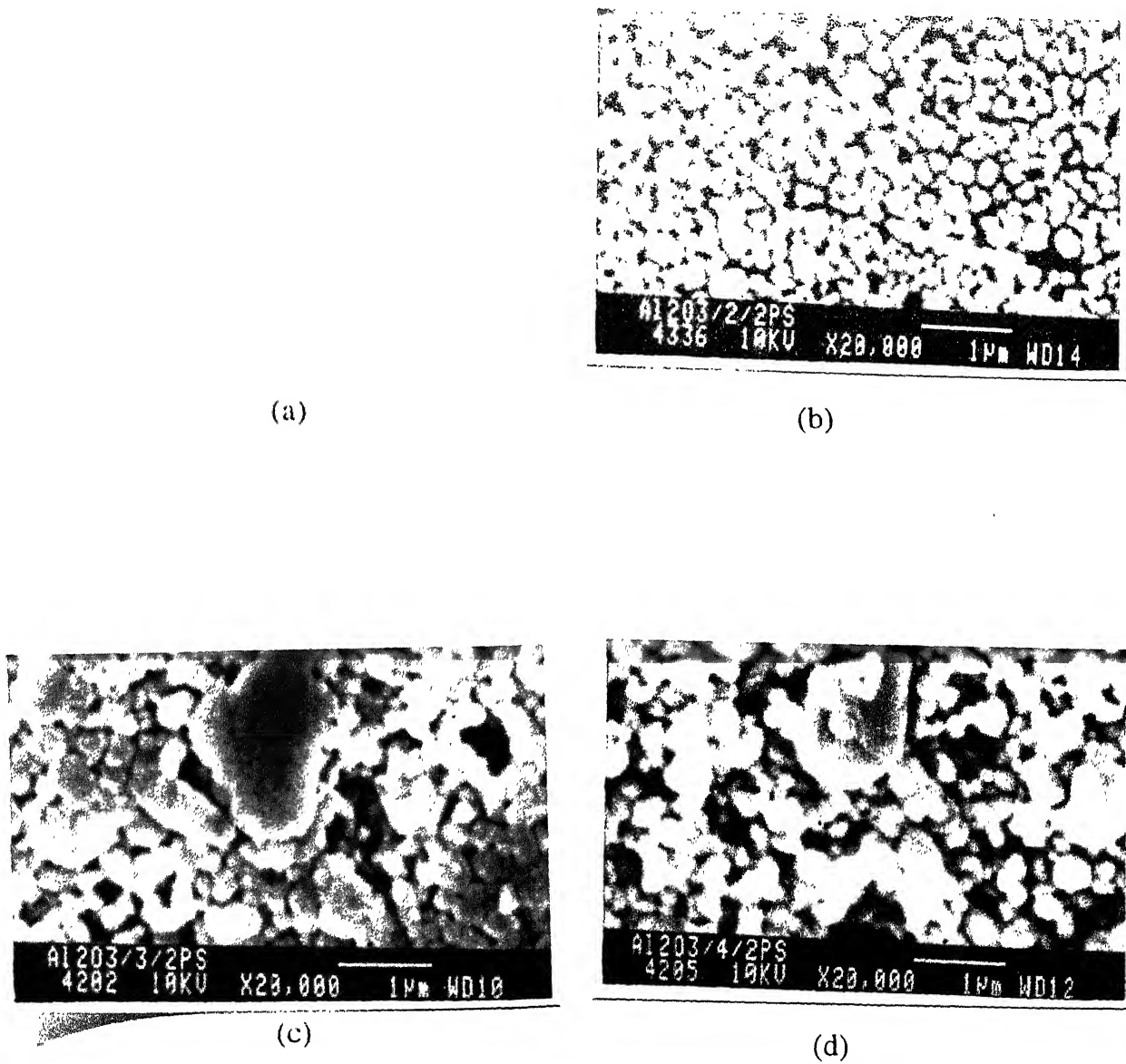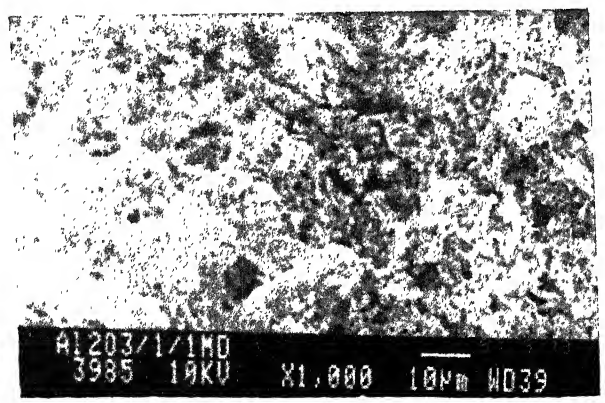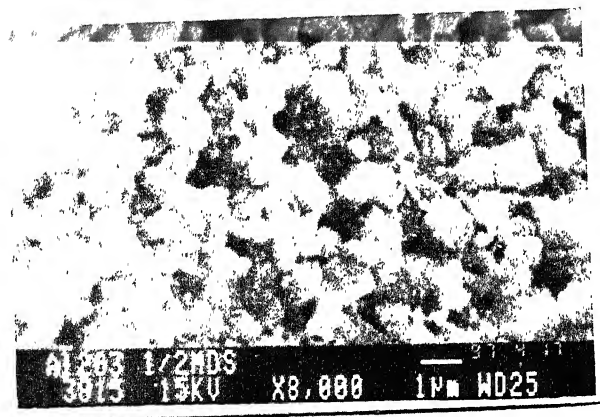
(a)

(b)

(c)

(d)

Figure 3.14: Polished surface (a) pure alumina not ground, (b)pure alumina ground, (c) alumina + 10% glass, (d) alumina + 20% glass
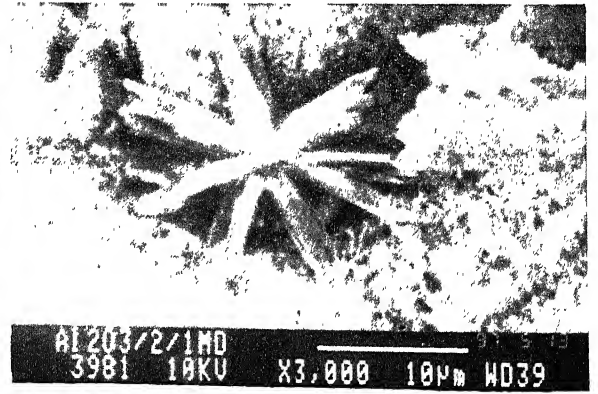
(a)

(b)

Figure 3.15: Machined surface of pure alumina not ground at two different magnifications, machining conditions (a) 50 V, 50^0C, (b) 60 V, 50^0C

(b)
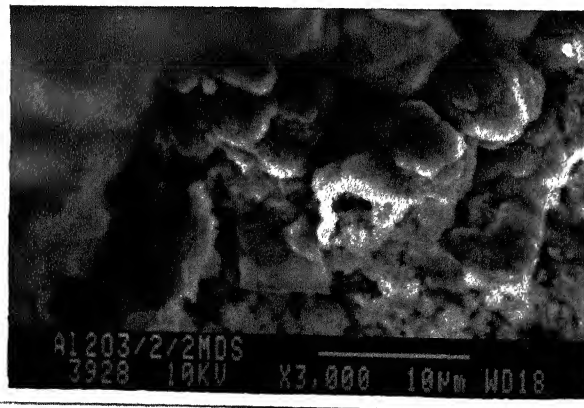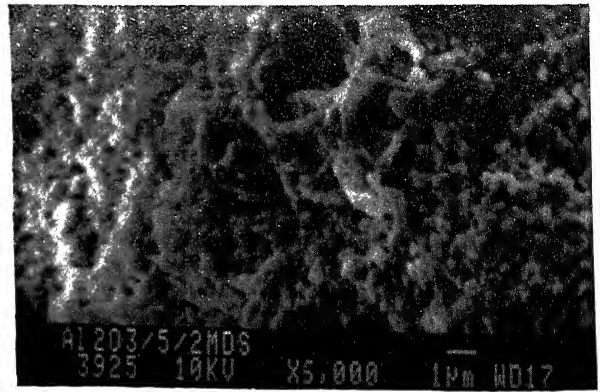

(c)

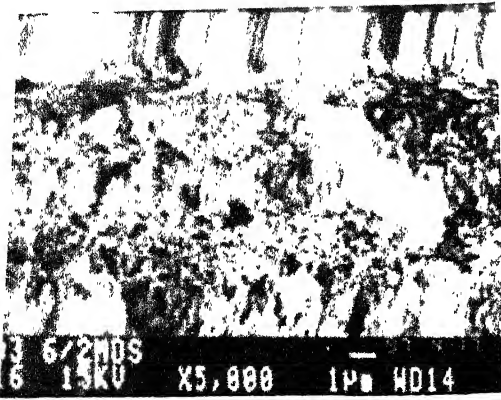Figure 3.16: Machined surface of pure alumina ground, machining conditions (a) 60 V, 50^0C, (b) 50 V, 50^0C,(c) 60 V, 50^0C
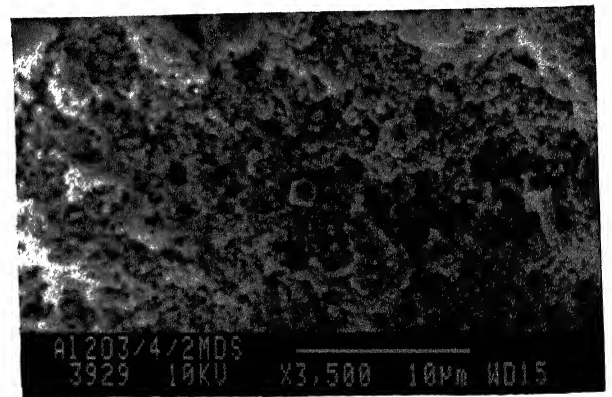
Figure 3.17: Machined surfaces of alumina samples having different amount of glass (a) 0.2 %, 60 V, $50^0 C$, (b) 0.2 %, 60 V, $50^0 C$, (c) 2.0 %, 60 V, $50^0 C$, (d) 10 %, 60 V,$50^0 C$ (e) 20 %, 50 v, $50^0 C$ (f) 20 %, 60 V, $50^0 C$

3.4 The Explanation for Typical Behaviour of Machining Performance Affected by Variable Parameters viz. Glass content, Porosity and Input Voltage

Aim of the experiment was to see the melting of the glassy phase present at the grain boundaries. Fig. (3.5) shows variations of material removal with porosity and glass. It can be seen that machining rate increases with porosity and decreases with increase in glass content except for the samples having 0 wt % of glass. The material removal appears be due to attack on the grain boundaries . Here a term "material removal front" is necessary to be defined. It is similar to the crack propagation front in the fracture due to the fatigue.The material removal front progresses along the grain boundaries. This process is slow. where a pore is encountered at the grain junctions, the front jumps across the pore. Thus there is an increase in the speed of the front due to the presence of the pore. This increase will be maximum if the average size and number density of the pore is higher . Thus increased porosity directly leads to an increase in MRR.

The effect of voltage on machining performance is explained on the basis that when input voltage is increased, the current drawn also increases resulting in higher intensity sparks. Thus, with increase in input voltage, material removal, machined depth and dimetral overcut are increased because the intensity of sparks is increased.
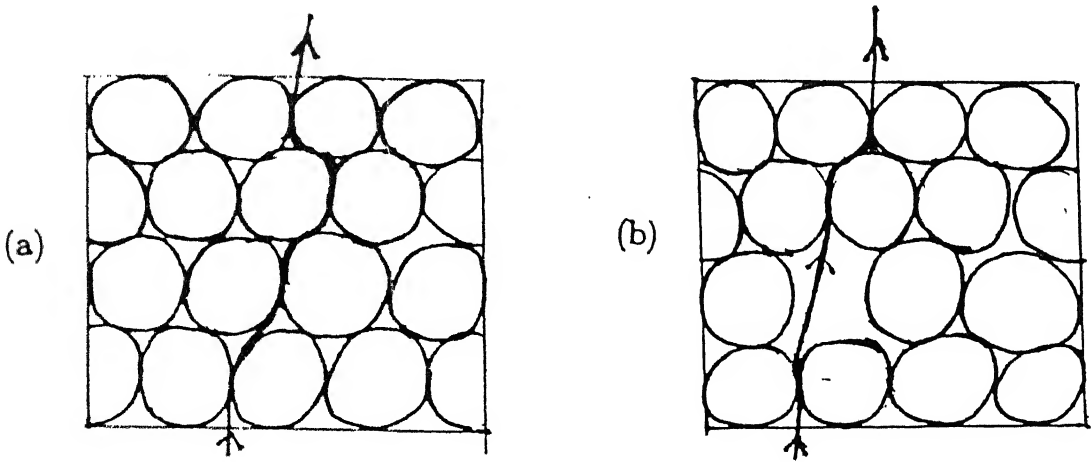
Figure 3.18: Material removal front propagation (a) for low porosity (b) for high porosity

3.5 Proposed Mechanism of Material Removal in Alumina

Alumina has high melting point (of the order of 2050^0C). So it requires a large amount of heat to melt alumina. From SEM photographs it seems that during machining of alumina by ECSM process , grains are being seperated from grain boundaries due to etching of grain boundaries in heated electrolyte. There is no exclusive clear evidence of melting of alumina as concluded from the SEM analysis of the machined surface.

Chapter 4

Concluding Remarks and Scope for Future Work

4.1   Conclusion

Results of the experiments are encouraging and have shown the possibility of further improvement in the process performance by improving existing setup. From the present work following conclusions are made.

1. Porosity of Alumina samples is the major governing factor of material removal and machining depth.

2. Machining of Alumina gives better machining accuracy at low voltage because at high voltage material shows cracking susceptibility.

3. Limitations on machining depth have been slightly relaxed in case of porous Alumina.

4. Maintaining the minimum gap between tool and workpiece has improved the efficiency of ECSM process.

5. If the glass added in Alumina acts as secondary phase particles then it reduces the machining performance of ECSM process.

6. SEM analysis has shown that quality of surface obtained is fairly good.

4.2   Scope for the Future Work

1. In order to study the effect of glass present at the grain boundaries, alumina samples of constant porosity should be prepared by 'sol-gel' method.

2. If the tool is exposed only at the bottom face and rest of tool is coated with insulator then it can give better machining accuracy of the samples.

3. Tool, workpiece and electrolyte should be kept in a closed vessel while machining because it will give the minimum evaporative loss of electrolyte and it will partially relax the limitation on the temperature of electrolyte.

4. Pulsed power supply with pulsed time of the order of micro seconds can improve the machining performance.

5. Use of combination of electrolytes has shown the better results. So it can improve the efficiency of ECSM process.

6. Study of the debris of the machined sample can give a better idea of process mechanism .

Bibliography

1. Jain V.K., Agrawal D.C., Singh Y.P., Kumar Prashant- "Machining piezoelectric ceramics using ECSM process", Journal of Material Processing Technology 58 (1996) 24-31.

2. Jain V.K., Rao P. Srinivasa, Choudhary S.K., Rajurkar K.P.- "Experimental investigation into travelling wire ECSM of composites", Trans. of ASME Journal of Engineering for Industry 113 (1991) 75-84.

3. Ni,X.W., McGeough, J. A.and Greated,C.A- "An optical study of electric discharge in electrochemical arc machining " Proceeding of Symposium on Research & Technology Developement in Nontraditional Machining, Rajurkar K.P. ed. 1988 PED vol (34), pp 63-73.

4. Kozak J. and Prusak M. - " Aspect of cutting by electrochemical arc machining", Proceeding of the International Symposium for Electromachining (ISEM-9) Nagoya, 1989, pp 103-106.

5. Ghosh A., Basak Indrajit - "Machanism of spark generation during electrochemical discharge machining , a theoritical model and experimental verification " Journal of Material Processing Technology 62 (1996) 46-53.

6. Gautam N. - "Experimental investigations for enhancement of ECDM process capabilities using various tool kinematics ", M Tech. Thesis IIT Kanpur 1995.

7. Chak S.K. - "Electrochemical spark machining of Alumina and Quartz ", M Tech. Thesis IIT Kanpur 1996.

8. Kellog H.H., Journal of Electrochemical Society n 97 pp 133, 1950.

9. Kurafugi H., Suda H. - "Electrical discharge drilling of glass" Annals of CIRP, vol.-16/1 pp 415, 1968.

10. Cook N. H., Jordan P., Kalyani B.N. - "Experimental studies in electromachining ", Trans. of ASME, Journal of Engineering for Industry pp 945-950, 1973

11. Taylor H., Trans of Electrochemical Society, n 47, pp 301, 1925.

12. Crichton I.M., McGrough J.A. - "Studies of dischrge mechanism in electrochemicl Arc machining", Journal of Applied Electrochemistry 15, pp 113-119, 1985.

13. H.T. Suchiya, T. Inoue, and M. Miyazki- " Wire electrochemical discharge machining of glasses and ceramics", Proceedings of 5th International Conference on Production Engineering, Tokyo pp 413-417, 1984.

14. Allesu K., Umesh Kumar N., Muju M.K., Ghosh A. - " Some investigations in to spark machining of nonconducting materials", 12th AIMTDR Conference IIT Delhi 1986.

15. Hitoshi Tokura , IWAO Kandoh -"Ceramics materials processing by electrical discharge in electrolyte", Journal of Material Science, Vol.24, pp 991- 998, 1989.

16. Umesh Kumar N -"An experimental study of electrical machining of nonconducting materials.", M.Tech thesis IIT Kanpur,1985

17. V. Raghuram, T. Pramila, Y.G. Srinivasa, K. Narayanswamy -"Effect of circuit parameters on the electrolytes in the electrochemical discharge phenomenon", Journal of Materials Processing Technology, Vol.52, pp 289-300, 1995.

18. I. Basak Ph. D. dessertion; IIT Kanpur,1992

19. N. Mohri, Y. Fukuzawa, T. Tani -"Assisting electrode method for machining insulating ceramics", Annals of the CIRP, Vol.45/1, pp 201-204, 1996.

20. Y. K. Loke and T.C. Lee -"Processing of advanced ceramics using the wirecut EDM process", Journal of Materials Processing Technology, Vol.63, pp 839-843, 1997.

21. Kumar S.-"Handbook of ceramics", Vol.1, 20B Dover Place, Calcutta .

22. Walter H.G.-"Alumina as a ceramic material", American ceramic society, Columbus, Ohio.

APPENDIX A

Mechanical Properties Of Alumina (Al_2O_3) [22].

Temperature in $^{\circ}C$	Compressive St. in psi	Tensile St. in psi	Impact Res. (ln - lb)
25	560,000[1]	*	1.2
25	426,000[2]	*	*
30	*	37,600	*
300	*	36,400	*
400	213,000	*	*
800	185,000	34,000	1.0
1000	128,000	*	0.55
1050	*	33,800	*
1100	*	31,400	*
1200	71,000	18,500	*
1400	35,600	4,250	*
1600	7,100	*	0.32

1 : Zero porosity

2 : Less than 5% porosity

$\star$: Data is not available

APPENDIX B

Thermal Properties Of Alumina (Al_2O_3) [22].

Melting Point : $2051.0 \pm 9.7^\circ C$

Boiling Point : $3530^\circ C (3800 \pm 200^\circ K)$

Temperature in $^\circ K$	Thermal Conductivity (cal/sec $cm^\circ C$)	Sp. Conductance (cal/$g^\circ K$)
298	0.086	*
373	0.069	*
400	*	0.22545
500	*	0.24857
573	0.038	*
600	*	0.26372
700	*	0.27431
773	0.025	*
800	*	0.28205
900	*	0.28789
973	0.018	*
1000	*	0.29240
1100	*	0.29595
1173	0.015	*
1200	*	0.2987
1373	0.014	*
1573	0.014	*
1773	0.013	*
1973	0.014	*
2173	0.015	*

123645

Date Slip

This book is to be returned on the
date last stamped.

123645